

# Neutrino Mixing

## (A) Accelerator neutrino experiments

$$\nu_e \rightarrow \nu_\tau$$

### $\Delta(m^2)$ for $\sin^2(2\theta) = 1$

VALUE (eV <sup>2</sup> )	CL%	DOCUMENT ID	TECN	COMMENT
<b>&lt; 0.77</b>	90	<sup>1</sup> ARMBRUSTER98	KARM	
● ● ● We do not use the following data for averages, fits, limits, etc. ● ● ●				
< 5.9	90	<sup>2</sup> ASTIER	01B NOMD	CERN SPS
< 7.5	90	<sup>3</sup> ESKUT	01 CHRS	CERN SPS
<17	90	NAPLES	99 CCFR	FNAL
<44	90	TALEBZADEH 87	HLBC	BEBC
< 9	90	USHIDA	86C EMUL	FNAL

<sup>1</sup> ARMBRUSTER 98 use KARMEN detector with  $\nu_e$  from muon decay at rest and observe  $^{12}\text{C}(\nu_e, e^-)^{12}\text{N}_{gs}$ . This is a disappearance experiment which is almost insensitive to  $\nu_e \rightarrow \nu_\mu$  oscillation. Results are presented as limits to  $\nu_e \rightarrow \nu_\tau$  oscillation, although the (non)oscillation could be to a non-visible flavor. A three-flavor analysis is also presented.

<sup>2</sup> ASTIER 01B searches for the appearance of  $\nu_\tau$  with the NOMAD detector at CERN's SPS. The limit is based on an oscillation probability  $< 0.74 \times 10^{-2}$ , whereas the quoted sensitivity was  $1.1 \times 10^{-2}$ . The limit was obtained following the statistical prescriptions of FELDMAN 98. See also the footnote to ESKUT 01.

<sup>3</sup> ESKUT 01 searches for the appearance of the  $\nu_\tau$  with the CHORUS detector at CERN's SPS. The limit is obtained following the statistical prescriptions in JUNK 99. The limit would have been  $6 \text{ eV}^2$  if the prescriptions in FELDMAN 98 had been followed, as they were in ASTIER 01B.

### $\sin^2(2\theta)$ for "Large" $\Delta(m^2)$

VALUE	CL%	DOCUMENT ID	TECN	COMMENT
<b>&lt;0.015</b>	90	<sup>4</sup> ASTIER	01B NOMD	CERN SPS
● ● ● We do not use the following data for averages, fits, limits, etc. ● ● ●				
<0.052	90	<sup>5</sup> ESKUT	01 CHRS	CERN SPS
<0.21	90	NAPLES	99 CCFR	FNAL
<0.338	90	<sup>6</sup> ARMBRUSTER98	KARM	
<0.36	90	TALEBZADEH 87	HLBC	BEBC
<0.25	90	<sup>7</sup> USHIDA	86C EMUL	FNAL

<sup>4</sup> ASTIER 01B limit is based on an oscillation probability  $< 0.74 \times 10^{-2}$ , whereas the quoted sensitivity was  $1.1 \times 10^{-2}$ . The limit was obtained following the statistical prescriptions of FELDMAN 98. See also the footnote to ESKUT 01.

<sup>5</sup> ESKUT 01 limit obtained following the statistical prescriptions in JUNK 99. The limit would have been 0.03 if the prescriptions in FELDMAN 98 had been followed, as they were in ASTIER 01B.

<sup>6</sup> See footnote in preceding table (ARMBRUSTER 98) for further details, and see the paper for a plot showing allowed regions. A three-flavor analysis is also presented here.

<sup>7</sup> USHIDA 86C published result is  $\sin^2 2\theta < 0.12$ . The quoted result is corrected for a numerical mistake incurred in calculating the expected number of  $\nu_e$  CC events, normalized to the total number of neutrino interactions (3886) rather than to the total number of  $\nu_\mu$  CC events (1870).

—————  $\bar{\nu}_e \rightarrow \bar{\nu}_\tau$  —————

**$\sin^2(2\theta)$  for “Large”  $\Delta(m^2)$**

<u>VALUE</u>	<u>CL%</u>	<u>DOCUMENT ID</u>	<u>TECN</u>	<u>COMMENT</u>
<b>&lt;0.7</b>	90	<sup>8</sup> FRITZE	80 HYBR	BEBC CERN SPS

<sup>8</sup> Authors give  $P(\nu_e \rightarrow \nu_\tau) < 0.35$ , equivalent to above limit.

—————  $\nu_e \nrightarrow \nu_e$  —————

**$\Delta(m^2)$  for  $\sin^2(2\theta) = 1$**

<u>VALUE (eV<sup>2</sup>)</u>	<u>CL%</u>	<u>DOCUMENT ID</u>	<u>TECN</u>	<u>COMMENT</u>
<b>&lt; 0.18</b>	90	<sup>9</sup> HAMPEL	98 GALX	<sup>51</sup> Cr source
• • • We do not use the following data for averages, fits, limits, etc. • • •				
<40	90	<sup>10</sup> BORISOV	96 CNTR	IHEP-JINR detector
<14.9	90	BRUCKER	86 HLBC	15-ft FNAL
< 8	90	BAKER	81 HLBC	15-ft FNAL
<56	90	DEDEN	81 HLBC	BEBC CERN SPS
<10	90	ERRIQUEZ	81 HLBC	BEBC CERN SPS
<2.3 OR >8	90	NEMETHY	81B CNTR	LAMPF

<sup>9</sup> HAMPEL 98 analyzed the GALLEX calibration results with <sup>51</sup>Cr neutrino sources and updates the BAHCALL 95 analysis result. They also gave 95% and 99% CL limits of < 0.2 and < 0.22, respectively.

<sup>10</sup> BORISOV 96 exclusion curve extrapolated to obtain this value; however, it does not have the right curvature in this region.

**$\sin^2(2\theta)$  for “Large”  $\Delta(m^2)$**

<u>VALUE</u>	<u>CL%</u>	<u>DOCUMENT ID</u>	<u>TECN</u>	<u>COMMENT</u>
<b>&lt;7 × 10<sup>-2</sup></b>	90	<sup>11</sup> ERRIQUEZ	81 HLBC	BEBC CERN SPS
• • • We do not use the following data for averages, fits, limits, etc. • • •				
<0.4	90	<sup>12</sup> HAMPEL	98 GALX	<sup>51</sup> Cr source
<0.115	90	<sup>13</sup> BORISOV	96 CNTR	$\Delta(m^2) = 175 \text{ eV}^2$
<0.54	90	BRUCKER	86 HLBC	15-ft FNAL
<0.6	90	BAKER	81 HLBC	15-ft FNAL
<0.3	90	<sup>11</sup> DEDEN	81 HLBC	BEBC CERN SPS

<sup>11</sup> Obtained from a Gaussian centered in the unphysical region.

<sup>12</sup> HAMPEL 98 analyzed the GALLEX calibration results with <sup>51</sup>Cr neutrino sources and updates the BAHCALL 95 analysis result. They also gave 95% and 99% CL limits of < 0.45 and < 0.56, respectively.

<sup>13</sup> BORISOV 96 sets less stringent limits at large  $\Delta(m^2)$ , but exclusion curve does not have clear asymptotic behavior.

—————  $\nu_e \rightarrow (\bar{\nu}_e)_L$  —————

This is a limit on lepton family-number violation and total lepton-number violation.  $(\bar{\nu}_e)_L$  denotes a hypothetical left-handed  $\bar{\nu}_e$ . The bound is quoted in terms of  $\Delta(m^2)$ ,  $\sin(2\theta)$ , and  $\alpha$ , where  $\alpha$  denotes the fractional admixture of (V+A) charged current.

**$\alpha\Delta(m^2)$  for  $\sin^2(2\theta) = 1$**

<u>VALUE (eV<sup>2</sup>)</u>	<u>CL%</u>	<u>DOCUMENT ID</u>	<u>TECN</u>	<u>COMMENT</u>
<b>&lt;0.14</b>	90	<sup>14</sup> FREEDMAN	93 CNTR	LAMPF

• • • We do not use the following data for averages, fits, limits, etc. • • •

<7 90 <sup>15</sup> COOPER 82 HLBC BEBC CERN SPS

<sup>14</sup> FREEDMAN 93 is a search at LAMPF for  $\bar{\nu}_e$  generated from any of the three neutrino types  $\nu_\mu$ ,  $\bar{\nu}_\mu$ , and  $\nu_e$  which come from the beam stop. The  $\bar{\nu}_e$ 's would be detected by the reaction  $\bar{\nu}_e p \rightarrow e^+ n$ .

<sup>15</sup> COOPER 82 states that existing bounds on V+A currents require  $\alpha$  to be small.

### $\alpha^2 \sin^2(2\theta)$ for "Large" $\Delta(m^2)$

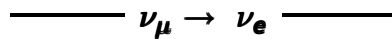
VALUE	CL%	DOCUMENT ID	TECN	COMMENT
<0.032	90	<sup>16</sup> FREEDMAN 93	CNTR	LAMPF

• • • We do not use the following data for averages, fits, limits, etc. • • •

<0.05 90 <sup>17</sup> COOPER 82 HLBC BEBC CERN SPS

<sup>16</sup> FREEDMAN 93 is a search at LAMPF for  $\bar{\nu}_e$  generated from any of the three neutrino types  $\nu_\mu$ ,  $\bar{\nu}_\mu$ , and  $\nu_e$  which come from the beam stop. The  $\bar{\nu}_e$ 's would be detected by the reaction  $\bar{\nu}_e p \rightarrow e^+ n$ .

<sup>17</sup> COOPER 82 states that existing bounds on V+A currents require  $\alpha$  to be small.



### $\Delta(m^2)$ for $\sin^2(2\theta) = 1$

VALUE (eV <sup>2</sup> )	CL%	DOCUMENT ID	TECN	COMMENT
<0.09	90	ANGELINI 86	HLBC	BEBC CERN PS

• • • We do not use the following data for averages, fits, limits, etc. • • •

		<sup>18</sup> AGUILAR 01	LSND	$\nu_\mu \rightarrow \nu_e$ osc.prob.
0.03 to 0.3	95	<sup>19</sup> ATHANASSO...98	LSND	$\nu_\mu \rightarrow \nu_e$
<2.3	90	<sup>20</sup> LOVERRE 96		CHARM/CDHS
<0.9	90	VILAIN 94C	CHM2	CERN SPS
<0.1	90	BLUMENFELD 89	CNTR	
<1.3	90	AMMOISOV 88	HLBC	SKAT at Serpukhov
<0.19	90	BERGSMA 88	CHRM	
		<sup>21</sup> LOVERRE 88	RVUE	
<2.4	90	AHRENS 87	CNTR	BNL AGS
<1.8	90	BOFILL 87	CNTR	FNAL
<2.2	90	<sup>22</sup> BRUCKER 86	HLBC	15-ft FNAL
<0.43	90	AHRENS 85	CNTR	BNL AGS E734
<0.20	90	BERGSMA 84	CHRM	
<1.7	90	ARMENISE 81	HLBC	GGM CERN PS
<0.6	90	BAKER 81	HLBC	15-ft FNAL
<1.7	90	ERRIQUEZ 81	HLBC	BEBC CERN PS
<1.2	95	BLIETSCHAU 78	HLBC	GGM CERN PS
<1.2	95	BELLOTTI 76	HLBC	GGM CERN PS

<sup>18</sup> AGUILAR 01 is the final analysis of the LSND full data set. Search is made for the  $\nu_\mu \rightarrow \nu_e$  oscillations using  $\nu_\mu$  from  $\pi^+$  decay in flight by observing beam-on electron events from  $\nu_e C \rightarrow e^- X$ . Present analysis results in  $8.1 \pm 12.2 \pm 1.7$  excess events in the  $60 < E_e < 200$  MeV energy range, corresponding to oscillation probability of  $0.10 \pm 0.16 \pm 0.04\%$ . This is consistent, though less significant, with the previous result of ATHANASSOPOULOS 98, which it supersedes. The present analysis uses selection criteria developed for the decay at rest region, and is less effective in removing the background above 60 MeV than ATHANASSOPOULOS 98.

- <sup>19</sup> ATHANASSOPOULOS 98 is a search for the  $\nu_\mu \rightarrow \nu_e$  oscillations using  $\nu_\mu$  from  $\pi^+$  decay in flight. The 40 observed beam-on electron events are consistent with  $\nu_e C \rightarrow e^- X$ ; the expected background is  $21.9 \pm 2.1$ . Authors interpret this excess as evidence for an oscillation signal corresponding to oscillations with probability  $(0.26 \pm 0.10 \pm 0.05)\%$ . Although the significance is only  $2.3\sigma$ , this measurement is an important and consistent cross check of ATHANASSOPOULOS 96 who reported evidence for  $\bar{\nu}_\mu \rightarrow \bar{\nu}_e$  oscillations from  $\mu^+$  decay at rest. See also ATHANASSOPOULOS 98B.
- <sup>20</sup> LOVERRE 96 uses the charged-current to neutral-current ratio from the combined CHARM (ALLABY 86) and CDHS (ABRAMOWICZ 86) data from 1986.
- <sup>21</sup> LOVERRE 88 reports a less stringent, indirect limit based on theoretical analysis of neutral to charged current ratios.
- <sup>22</sup> 15ft bubble chamber at FNAL.

### $\sin^2(2\theta)$ for "Large" $\Delta(m^2)$

VALUE (units $10^{-3}$ )	CL%	DOCUMENT ID	TECN	COMMENT
< 3.0	90	<sup>23</sup> LOVERRE 96		CHARM/CDHS
< 2.5	90	AMMOISOV 88	HLBC	SKAT at Serpukhov
● ● ● We do not use the following data for averages, fits, limits, etc. ● ● ●				
0.0005 to 0.03	95	<sup>24</sup> AGUILAR 01	LSND	$\nu_\mu \rightarrow \nu_e$ osc.prob.
		<sup>25</sup> ATHANASSO...98	LSND	$\nu_\mu \rightarrow \nu_e$
< 9.4	90	VILAIN 94C	CHM2	CERN SPS
< 5.6	90	<sup>26</sup> VILAIN 94C	CHM2	CERN SPS
< 16	90	BLUMENFELD 89	CNTR	
< 8	90	BERGSMA 88	CHRM	$\Delta(m^2) \geq 30 \text{ eV}^2$
		<sup>27</sup> LOVERRE 88	RVUE	
< 10	90	AHRENS 87	CNTR	BNL AGS
< 15	90	BOFILL 87	CNTR	FNAL
< 20	90	<sup>28</sup> ANGELINI 86	HLBC	BEBC CERN PS
20 to 40		<sup>29</sup> BERNARDI 86B	CNTR	$\Delta(m^2)=5-10$
< 11	90	<sup>30</sup> BRUCKER 86	HLBC	15-ft FNAL
< 3.4	90	AHRENS 85	CNTR	BNL AGS E734
< 240	90	BERGSMA 84	CHRM	
< 10	90	ARMENISE 81	HLBC	GGM CERN PS
< 6	90	BAKER 81	HLBC	15-ft FNAL
< 10	90	ERRIQUEZ 81	HLBC	BEBC CERN PS
< 4	95	BLIETSCHAU 78	HLBC	GGM CERN PS
< 10	95	BELLOTTI 76	HLBC	GGM CERN PS

- <sup>23</sup> LOVERRE 96 uses the charged-current to neutral-current ratio from the combined CHARM (ALLABY 86) and CDHS (ABRAMOWICZ 86) data from 1986.
- <sup>24</sup> AGUILAR 01 is the final analysis of the LSND full data set of the search for the  $\nu_\mu \rightarrow \nu_e$  oscillations. See footnote in preceding table for further details.
- <sup>25</sup> ATHANASSOPOULOS 98 report  $(0.26 \pm 0.10 \pm 0.05)\%$  for the oscillation probability; the value of  $\sin^2 2\theta$  for large  $\Delta m^2$  is deduced from this probability. See footnote in preceding table for further details, and see the paper for a plot showing allowed regions. If effect is due to oscillation, it is most likely to be intermediate  $\sin^2 2\theta$  and  $\Delta m^2$ . See also ATHANASSOPOULOS 98B.
- <sup>26</sup> VILAIN 94C limit derived by combining the  $\nu_\mu$  and  $\bar{\nu}_\mu$  data assuming  $CP$  conservation.
- <sup>27</sup> LOVERRE 88 reports a less stringent, indirect limit based on theoretical analysis of neutral to charged current ratios.
- <sup>28</sup> ANGELINI 86 limit reaches  $13 \times 10^{-3}$  at  $\Delta(m^2) \approx 2 \text{ eV}^2$ .

- <sup>29</sup> BERNARDI 86B is a typical fit to the data, assuming mixing between two species. As the authors state, this result is in conflict with earlier upper bounds on this type of neutrino oscillations.  
<sup>30</sup> 15ft bubble chamber at FNAL.

$$\text{----- } \bar{\nu}_\mu \rightarrow \bar{\nu}_e \text{ -----}$$

### $\Delta(m^2)$ for $\sin^2(2\theta) = 1$

VALUE (eV <sup>2</sup> )	CL%	DOCUMENT ID	TECN	COMMENT
<b>&lt;0.14</b>	90	<sup>31</sup> FREEDMAN	93 CNTR	LAMPF
• • • We do not use the following data for averages, fits, limits, etc. • • •				
0.03–0.05		<sup>32</sup> AGUILAR	01 LSND	LAMPF
0.05–0.08	90	<sup>33</sup> ATHANASSO...96	LSND	LAMPF
0.048–0.090	80	<sup>34</sup> ATHANASSO...95		
<0.07	90	<sup>35</sup> HILL	95	
<0.9	90	VILAIN	94C CHM2	CERN SPS
<3.1	90	BOFILL	87 CNTR	FNAL
<2.4	90	TAYLOR	83 HLBC	15-ft FNAL
<0.91	90	<sup>36</sup> NEMETHY	81B CNTR	LAMPF
<1	95	BLIETSCHAU	78 HLBC	GGM CERN PS

- <sup>31</sup> FREEDMAN 93 is a search at LAMPF for  $\bar{\nu}_e$  generated from any of the three neutrino types  $\nu_\mu$ ,  $\bar{\nu}_\mu$ , and  $\nu_e$  which come from the beam stop. The  $\bar{\nu}_e$ 's would be detected by the reaction  $\bar{\nu}_e p \rightarrow e^+ n$ . FREEDMAN 93 replaces DURKIN 88.
- <sup>32</sup> AGUILAR 01 is the final analysis of the LSND full data set. It is a search for  $\bar{\nu}_e$  30 m from LAMPF beam stop. Neutrinos originate mainly for  $\pi^+$  decay at rest.  $\bar{\nu}_e$  are detected through  $\bar{\nu}_e p \rightarrow e^+ n$  ( $20 < E_{e^+} < 60$  MeV) in delayed coincidence with  $np \rightarrow d\gamma$ . Authors observe  $87.9 \pm 22.4 \pm 6.0$  total excess events. The observation is attributed to  $\bar{\nu}_\mu \rightarrow \bar{\nu}_e$  oscillations with the oscillation probability of  $0.264 \pm 0.067 \pm 0.045\%$ , consistent with the previously published result. Taking into account all constraints, the most favored allowed region of oscillation parameters is a band of  $\Delta(m^2)$  from 0.2–2.0 eV<sup>2</sup>. Supersedes ATHANASSOPOULOS 95, ATHANASSOPOULOS 96, and ATHANASSOPOULOS 98.
- <sup>33</sup> ATHANASSOPOULOS 96 is a search for  $\bar{\nu}_e$  30 m from LAMPF beam stop. Neutrinos originate mainly from  $\pi^+$  decay at rest.  $\bar{\nu}_e$  could come from either  $\bar{\nu}_\mu \rightarrow \bar{\nu}_e$  or  $\nu_e \rightarrow \bar{\nu}_e$ ; our entry assumes the first interpretation. They are detected through  $\bar{\nu}_e p \rightarrow e^+ n$  ( $20 \text{ MeV} < E_{e^+} < 60 \text{ MeV}$ ) in delayed coincidence with  $np \rightarrow d\gamma$ . Authors observe  $51 \pm 20 \pm 8$  total excess events over an estimated background  $12.5 \pm 2.9$ . ATHANASSOPOULOS 96B is a shorter version of this paper.
- <sup>34</sup> ATHANASSOPOULOS 95 error corresponds to the  $1.6\sigma$  band in the plot. The expected background is  $2.7 \pm 0.4$  events. Corresponds to an oscillation probability of  $(0.34^{+0.20}_{-0.18} \pm 0.07)\%$ . For a different interpretation, see HILL 95. Replaced by ATHANASSOPOULOS 96.
- <sup>35</sup> HILL 95 is a report by one member of the LSND Collaboration, reporting a different conclusion from the analysis of the data of this experiment (see ATHANASSOPOULOS 95). Contrary to the rest of the LSND Collaboration, Hill finds no evidence for the neutrino oscillation  $\bar{\nu}_\mu \rightarrow \bar{\nu}_e$  and obtains only upper limits.
- <sup>36</sup> In reaction  $\bar{\nu}_e p \rightarrow e^+ n$ .

### $\sin^2(2\theta)$ for "Large" $\Delta(m^2)$

<u>VALUE</u>	<u>CL%</u>	<u>DOCUMENT ID</u>	<u>TECN</u>	<u>COMMENT</u>
<b>&lt;0.004</b>	95	BLIETSCHAU 78	HLBC	GGM CERN PS
● ● ● We do not use the following data for averages, fits, limits, etc. ● ● ●				
0.0053 ± 0.0013 ± 0.009		<sup>37</sup> AGUILAR 01	LSND	LAMPF
0.0062 ± 0.0024 ± 0.0010		<sup>38</sup> ATHANASSO...96	LSND	LAMPF
0.003–0.012	80	<sup>39</sup> ATHANASSO...95		
<0.006	90	<sup>40</sup> HILL 95		
<4.8	90	VILAIN 94C	CHM2	CERN SPS
<5.6	90	<sup>41</sup> VILAIN 94C	CHM2	CERN SPS
<0.024	90	<sup>42</sup> FREEDMAN 93	CNTR	LAMPF
<0.04	90	BOFILL 87	CNTR	FNAL
<0.013	90	TAYLOR 83	HLBC	15-ft FNAL
<0.2	90	<sup>43</sup> NEMETHY 81B	CNTR	LAMPF

<sup>37</sup> AGUILAR 01 is the final analysis of the LSND full data set. The deduced oscillation probability is  $0.264 \pm 0.067 \pm 0.045\%$ ; the value of  $\sin^2 2\theta$  for large  $\Delta(m^2)$  is twice this probability (although these values are excluded by other constraints). See footnote in preceding table for further details, and the paper for a plot showing allowed regions. Supersedes ATHANASSOPOULOS 95, ATHANASSOPOULOS 96, and ATHANASSOPOULOS 98.

<sup>38</sup> ATHANASSOPOULOS 96 reports  $(0.31 \pm 0.12 \pm 0.05)\%$  for the oscillation probability; the value of  $\sin^2 2\theta$  for large  $\Delta(m^2)$  should be twice this probability. See footnote in preceding table for further details, and see the paper for a plot showing allowed regions.

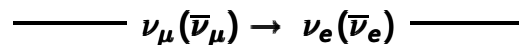
<sup>39</sup> ATHANASSOPOULOS 95 error corresponds to the  $1.6\sigma$  band in the plot. The expected background is  $2.7 \pm 0.4$  events. Corresponds to an oscillation probability of  $(0.34^{+0.20}_{-0.18} \pm 0.07)\%$ . For a different interpretation, see HILL 95. Replaced by ATHANASSOPOULOS 96.

<sup>40</sup> HILL 95 is a report by one member of the LSND Collaboration, reporting a different conclusion from the analysis of the data of this experiment (see ATHANASSOPOULOS 95). Contrary to the rest of the LSND Collaboration, Hill finds no evidence for the neutrino oscillation  $\bar{\nu}_\mu \rightarrow \bar{\nu}_e$  and obtains only upper limits.

<sup>41</sup> VILAIN 94C limit derived by combining the  $\nu_\mu$  and  $\bar{\nu}_\mu$  data assuming  $CP$  conservation.

<sup>42</sup> FREEDMAN 93 is a search at LAMPF for  $\bar{\nu}_e$  generated from any of the three neutrino types  $\nu_\mu$ ,  $\bar{\nu}_\mu$ , and  $\nu_e$  which come from the beam stop. The  $\bar{\nu}_e$ 's would be detected by the reaction  $\bar{\nu}_e p \rightarrow e^+ n$ . FREEDMAN 93 replaces DURKIN 88.

<sup>43</sup> In reaction  $\bar{\nu}_e p \rightarrow e^+ n$ .



### $\Delta(m^2)$ for $\sin^2(2\theta) = 1$

<u>VALUE (eV<sup>2</sup>)</u>	<u>CL%</u>	<u>DOCUMENT ID</u>	<u>TECN</u>	<u>COMMENT</u>
<b>&lt;0.075</b>	90	BORODOV... 92	CNTR	BNL E776
● ● ● We do not use the following data for averages, fits, limits, etc. ● ● ●				
<1.6	90	<sup>44</sup> ROMOSAN 97	CCFR	FNAL

<sup>44</sup> ROMOSAN 97 uses wideband beam with a 0.5 km decay region.

## $\sin^2(2\theta)$ for "Large" $\Delta(m^2)$

VALUE (units $10^{-3}$ )	CL%	DOCUMENT ID	TECN	COMMENT
<b>&lt;1.8</b>	90	<sup>45</sup> ROMOSAN	97 CCFR	FNAL
<3.8	90	<sup>46</sup> MCFARLAND	95 CCFR	FNAL
<3	90	BORODOV...	92 CNTR	BNL E776

• • • We do not use the following data for averages, fits, limits, etc. • • •

<sup>45</sup> ROMOSAN 97 uses wideband beam with a 0.5 km decay region.

<sup>46</sup> MCFARLAND 95 state that "This result is the most stringent to date for  $250 < \Delta(m^2) < 450 \text{ eV}^2$  and also excludes at 90%CL much of the high  $\Delta(m^2)$  region favored by the recent LSND observation." See ATHANASSOPOULOS 95 and ATHANASSOPOULOS 96.

$$\nu_\mu \rightarrow \nu_\tau$$

## $\Delta(m^2)$ for $\sin^2(2\theta) = 1$

VALUE ( $\text{eV}^2$ )	CL%	DOCUMENT ID	TECN	COMMENT
<b>&lt; 0.6</b>	90	<sup>47</sup> ESKUT	01 CHRS	CERN SPS
< 0.7	90	<sup>48</sup> ASTIER	01B NOMD	CERN SPS
< 1.4	90	<sup>49</sup> ALTEGOER	98B NOMD	CERN SPS
< 1.5	90	<sup>50</sup> ESKUT	98 CHRS	CERN SPS
< 1.1	90	<sup>51</sup> ESKUT	98B CHRS	CERN SPS
< 3.3	90	<sup>52</sup> LOVERRE	96	CHARM/CDHS
< 1.4	90	MCFARLAND	95 CCFR	FNAL
< 4.5	90	BATUSOV	90B EMUL	FNAL
<10.2	90	BOFILL	87 CNTR	FNAL
< 6.3	90	BRUCKER	86 HLBC	15-ft FNAL
< 0.9	90	USHIDA	86C EMUL	FNAL
< 4.6	90	ARMENISE	81 HLBC	GGM CERN SPS
< 3	90	BAKER	81 HLBC	15-ft FNAL
< 6	90	ERRIQUEZ	81 HLBC	BEBC CERN SPS
< 3	90	USHIDA	81 EMUL	FNAL

• • • We do not use the following data for averages, fits, limits, etc. • • •

<sup>47</sup> ESKUT 01 limit obtained following the statistical prescriptions in JUNK 99. The limit would have been  $0.5 \text{ eV}^2$  if the prescriptions in FELDMAN 98 had been followed, as they were in ASTIER 01B.

<sup>48</sup> ASTIER 01B limit is based on an oscillation probability  $< 1.63 \times 10^{-4}$ , whereas the quoted sensitivity was  $2.5 \times 10^{-4}$ . The limit was obtained following the statistical prescriptions of FELDMAN 98. See also the footnote to ESKUT 01.

<sup>49</sup> ALTEGOER 98B is the NOMAD 1995 data sample result, searching for events with  $\tau^- \rightarrow e^- \nu_\tau \bar{\nu}_e$ ,  $\text{hadron}^- \nu_\tau$ , or  $\pi^- \pi^+ \pi^-$  decay modes using classical CL approach of FELDMAN 98.

<sup>50</sup> ESKUT 98 search for events with one  $\mu^-$  with indication of a kink from  $\tau^-$  decay in the nuclear emulsion. No candidates were found in a 31,423 event subsample.

<sup>51</sup> ESKUT 98B search for  $\tau^- \rightarrow \mu^- \nu_\tau \bar{\nu}_\mu$  or  $h^- \nu_\tau \bar{\nu}_\mu$ , where  $h^-$  is a negatively charged hadron. The  $\mu^-$  sample is somewhat larger than in ESKUT 98, which this result supercedes. Bayesian limit.

<sup>52</sup> LOVERRE 96 uses the charged-current to neutral-current ratio from the combined CHARM (ALLABY 86) and CDHS (ABRAMOWICZ 86) data from 1986.

## $\sin^2(2\theta)$ for "Large" $\Delta(m^2)$

<u>VALUE</u>	<u>CL%</u>	<u>DOCUMENT ID</u>	<u>TECN</u>	<u>COMMENT</u>
<b>&lt;0.00033</b>	90	<sup>53</sup> ASTIER	01B	NOMD CERN SPS
● ● ● We do not use the following data for averages, fits, limits, etc. ● ● ●				
<0.00068	90	<sup>54</sup> ESKUT	01	CHRS CERN SPS
<0.0042	90	<sup>55</sup> ALTEGOER	98B	NOMD CERN SPS
<0.0035	90	<sup>56</sup> ESKUT	98	CHRS CERN SPS
<0.0018	90	<sup>57</sup> ESKUT	98B	CHRS CERN SPS
<0.006	90	<sup>58</sup> LOVERRE	96	CHARM/CDHS
<0.0081	90	MCFARLAND	95	CCFR FNAL
<0.06	90	BATUSOV	90B	EMUL FNAL
<0.34	90	BOFILL	87	CNTR FNAL
<0.088	90	BRUCKER	86	HLBC 15-ft FNAL
<0.004	90	USHIDA	86C	EMUL FNAL
<0.11	90	BALLAGH	84	HLBC 15-ft FNAL
<0.017	90	ARMENISE	81	HLBC GGM CERN SPS
<0.06	90	BAKER	81	HLBC 15-ft FNAL
<0.05	90	ERRIQUEZ	81	HLBC BEBC CERN SPS
<0.013	90	USHIDA	81	EMUL FNAL

<sup>53</sup> ASTIER 01B limit is based on an oscillation probability  $< 1.63 \times 10^{-4}$ , whereas the quoted sensitivity was  $2.5 \times 10^{-4}$ . The limit was obtained following the statistical prescriptions of FELDMAN 98. See also the footnote to ESKUT 01.

<sup>54</sup> ESKUT 01 limit obtained following the statistical prescriptions in JUNK 99. The limit would have been 0.00040 if the prescriptions in FELDMAN 98 had been followed, as they were in ASTIER 01B.

<sup>55</sup> ALTEGOER 98B is the NOMAD 1995 data sample result, searching for events with  $\tau^- \rightarrow e^- \nu_\tau \bar{\nu}_e$ ,  $\text{hadron}^- \nu_\tau$ , or  $\pi^- \pi^+ \pi^-$  decay modes using classical CL approach of FELDMAN 98.

<sup>56</sup> ESKUT 98 search for events with one  $\mu^-$  with indication of a kink from  $\tau^-$  decay in the nuclear emulsion. No candidates were found in a 31,423 event subsample.

<sup>57</sup> ESKUT 98B search for  $\tau^- \rightarrow \mu^- \nu_\tau \bar{\nu}_\mu$  or  $h^- \nu_\tau \bar{\nu}_\mu$ , where  $h^-$  is a negatively charged hadron. The  $\mu^-$  sample is somewhat larger than in ESKUT 98, which this result supercedes. Bayesian limit.

<sup>58</sup> LOVERRE 96 uses the charged-current to neutral-current ratio from the combined CHARM (ALLABY 86) and CDHS (ABRAMOWICZ 86) data from 1986.

$$\text{————— } \bar{\nu}_\mu \rightarrow \bar{\nu}_\tau \text{ —————}$$

## $\Delta(m^2)$ for $\sin^2(2\theta) = 1$

<u>VALUE (eV<sup>2</sup>)</u>	<u>CL%</u>	<u>DOCUMENT ID</u>	<u>TECN</u>	<u>COMMENT</u>
<b>&lt;2.2</b>	90	ASRATYAN	81	HLBC FNAL
● ● ● We do not use the following data for averages, fits, limits, etc. ● ● ●				
<1.4	90	MCFARLAND	95	CCFR FNAL
<6.5	90	BOFILL	87	CNTR FNAL
<7.4	90	TAYLOR	83	HLBC 15-ft FNAL



### $\sin^2(2\theta)$ for "Large" $\Delta(m^2)$

VALUE	CL%	DOCUMENT ID	TECN	COMMENT
<b>&lt;4.4</b> $\times 10^{-2}$	90	ASRATYAN	81	HLBC FNAL
● ● ● We do not use the following data for averages, fits, limits, etc. ● ● ●				
<0.0081	90	MCFARLAND	95	CCFR FNAL
<0.15	90	BOFILL	87	CNTR FNAL
<8.8 $\times 10^{-2}$	90	TAYLOR	83	HLBC 15-ft FNAL

$$\nu_\mu(\bar{\nu}_\mu) \rightarrow \nu_\tau(\bar{\nu}_\tau)$$

### $\Delta(m^2)$ for $\sin^2(2\theta) = 1$

VALUE (eV <sup>2</sup> )	CL%	DOCUMENT ID	TECN	COMMENT
<b>&lt;1.5</b>	90	<sup>59</sup> GRUWE	93	CHM2 CERN SPS

<sup>59</sup>GRUWE 93 is a search using the CHARM II detector in the CERN SPS wide-band neutrino beam for  $\nu_\mu \rightarrow \nu_\tau$  and  $\bar{\nu}_\mu \rightarrow \bar{\nu}_\tau$  oscillations signalled by quasi-elastic  $\nu_\tau$  and  $\bar{\nu}_\tau$  interactions followed by the decay  $\tau \rightarrow \nu_\tau \pi$ . The maximum sensitivity in  $\sin^2 2\theta$  ( $< 6.4 \times 10^{-3}$  at the 90% CL) is reached for  $\Delta(m^2) \simeq 50 \text{ eV}^2$ .

### $\sin^2(2\theta)$ for "Large" $\Delta(m^2)$

VALUE (units $10^{-3}$ )	CL%	DOCUMENT ID	TECN	COMMENT
<b>&lt;8</b>	90	<sup>60</sup> GRUWE	93	CHM2 CERN SPS

<sup>60</sup>GRUWE 93 is a search using the CHARM II detector in the CERN SPS wide-band neutrino beam for  $\nu_\mu \rightarrow \nu_\tau$  and  $\bar{\nu}_\mu \rightarrow \bar{\nu}_\tau$  oscillations signalled by quasi-elastic  $\nu_\tau$  and  $\bar{\nu}_\tau$  interactions followed by the decay  $\tau \rightarrow \nu_\tau \pi$ . The maximum sensitivity in  $\sin^2 2\theta$  ( $< 6.4 \times 10^{-3}$  at the 90% CL) is reached for  $\Delta(m^2) \simeq 50 \text{ eV}^2$ .

$$\nu_\mu \not\leftrightarrow \nu_\mu$$

### $\Delta(m^2)$ for $\sin^2(2\theta) = 1$

VALUE (eV <sup>2</sup> )	CL%	DOCUMENT ID	TECN	COMMENT
<b>&lt;0.23 OR &gt;1500 OUR LIMIT</b>				

<b>&lt;0.23 OR &gt;100</b>	90	DYDAK	84	CNTR
<b>&lt;13 OR &gt;1500</b>	90	STOCKDALE	84	CNTR
● ● ● We do not use the following data for averages, fits, limits, etc. ● ● ●				
< 0.29 OR >22	90	BERGSMA	88	CHRM
<7	90	BELIKOV	85	CNTR Serpukhov
<8.0 OR >1250	90	STOCKDALE	85	CNTR
<0.29 OR >22	90	BERGSMA	84	CHRM
<8.0	90	BELIKOV	83	CNTR

### $\sin^2(2\theta)$ for $\Delta(m^2) = 100\text{eV}^2$

VALUE	CL%	DOCUMENT ID	TECN	COMMENT
<b>&lt;0.02</b>	90	<sup>61</sup> STOCKDALE	85	CNTR FNAL

● ● ● We do not use the following data for averages, fits, limits, etc. ● ● ●				
<0.17	90	<sup>62</sup> BERGSMA	88	CHRM
<0.07	90	<sup>63</sup> BELIKOV	85	CNTR Serpukhov
<0.27	90	<sup>62</sup> BERGSMA	84	CHRM CERN PS
<0.1	90	<sup>64</sup> DYDAK	84	CNTR CERN PS
<0.02	90	<sup>65</sup> STOCKDALE	84	CNTR FNAL
<0.1	90	<sup>66</sup> BELIKOV	83	CNTR Serpukhov

- <sup>61</sup> This bound applies for  $\Delta(m^2) = 100 \text{ eV}^2$ . Less stringent bounds apply for other  $\Delta(m^2)$ ; these are nontrivial for  $8 < \Delta(m^2) < 1250 \text{ eV}^2$ .
- <sup>62</sup> This bound applies for  $\Delta(m^2) = 0.7\text{--}9. \text{ eV}^2$ . Less stringent bounds apply for other  $\Delta(m^2)$ ; these are nontrivial for  $0.28 < \Delta(m^2) < 22 \text{ eV}^2$ .
- <sup>63</sup> This bound applies for a wide range of  $\Delta(m^2) > 7 \text{ eV}^2$ . For some values of  $\Delta(m^2)$ , the value is less stringent; the least restrictive, nontrivial bound occurs approximately at  $\Delta(m^2) = 300 \text{ eV}^2$  where  $\sin^2(2\theta) < 0.13$  at CL = 90%.
- <sup>64</sup> This bound applies for  $\Delta(m^2) = 1\text{--}10. \text{ eV}^2$ . Less stringent bounds apply for other  $\Delta(m^2)$ ; these are nontrivial for  $0.23 < \Delta(m^2) < 90 \text{ eV}^2$ .
- <sup>65</sup> This bound applies for  $\Delta(m^2) = 110 \text{ eV}^2$ . Less stringent bounds apply for other  $\Delta(m^2)$ ; these are nontrivial for  $13 < \Delta(m^2) < 1500 \text{ eV}^2$ .
- <sup>66</sup> Bound holds for  $\Delta(m^2) = 20\text{--}1000 \text{ eV}^2$ .

$$\text{————— } \bar{\nu}_\mu \not\leftrightarrow \bar{\nu}_\mu \text{ —————}$$

### $\Delta(m^2)$ for $\sin^2(2\theta) = 1$

VALUE (eV <sup>2</sup> )	CL%	DOCUMENT ID	TECN
<b>&lt;7 OR &gt;1200 OUR LIMIT</b>			
<b>&lt;7 OR &gt;1200</b>	90	STOCKDALE 85	CNTR

### $\sin^2(2\theta)$ for $190 \text{ eV}^2 < \Delta(m^2) < 320 \text{ eV}^2$

VALUE	CL%	DOCUMENT ID	TECN	COMMENT
<b>&lt;0.02</b>	90	<sup>67</sup> STOCKDALE 85	CNTR	FNAL

- <sup>67</sup> This bound applies for  $\Delta(m^2)$  between 190 and 320 or = 530 eV<sup>2</sup>. Less stringent bounds apply for other  $\Delta(m^2)$ ; these are nontrivial for  $7 < \Delta(m^2) < 1200 \text{ eV}^2$ .

$$\text{————— } \nu_\mu \rightarrow (\bar{\nu}_e)_L \text{ —————}$$

See note above for  $\nu_e \rightarrow (\bar{\nu}_e)_L$  limit

### $\alpha\Delta(m^2)$ for $\sin^2(2\theta) = 1$

VALUE (eV <sup>2</sup> )	CL%	DOCUMENT ID	TECN	COMMENT
<b>&lt;0.16</b>	90	<sup>68</sup> FREEDMAN 93	CNTR	LAMPF

- • • We do not use the following data for averages, fits, limits, etc. • • •

<0.7	90	<sup>69</sup> COOPER 82	HLBC	BECB CERN SPS
------	----	-------------------------	------	---------------

- <sup>68</sup> FREEDMAN 93 is a search at LAMPF for  $\bar{\nu}_e$  generated from any of the three neutrino types  $\nu_\mu, \bar{\nu}_\mu,$  and  $\nu_e$  which come from the beam stop. The  $\bar{\nu}_e$ 's would be detected by the reaction  $\bar{\nu}_e p \rightarrow e^+ n$ . The limit on  $\Delta(m^2)$  is better than the CERN BECB experiment, but the limit on  $\sin^2\theta$  is almost a factor of 100 less sensitive.

- <sup>69</sup> COOPER 82 states that existing bounds on V+A currents require  $\alpha$  to be small.

### $\alpha^2\sin^2(2\theta)$ for "Large" $\Delta(m^2)$

VALUE	CL%	DOCUMENT ID	TECN	COMMENT
<b>&lt;0.001</b>	90	<sup>70</sup> COOPER 82	HLBC	BECB CERN SPS

- • • We do not use the following data for averages, fits, limits, etc. • • •

<0.07	90	<sup>71</sup> FREEDMAN 93	CNTR	LAMPF
-------	----	---------------------------	------	-------

<sup>70</sup> COOPER 82 states that existing bounds on V+A currents require  $\alpha$  to be small.

<sup>71</sup> FREEDMAN 93 is a search at LAMPF for  $\bar{\nu}_e$  generated from any of the three neutrino types  $\nu_\mu$ ,  $\bar{\nu}_\mu$ , and  $\nu_e$  which come from the beam stop. The  $\bar{\nu}_e$ 's would be detected by the reaction  $\bar{\nu}_e p \rightarrow e^+ n$ . The limit on  $\Delta(m^2)$  is better than the CERN BEBC experiment, but the limit on  $\sin^2\theta$

## (B) Reactor $\bar{\nu}_e$ disappearance experiments

In most cases, the reaction  $\bar{\nu}_e p \rightarrow e^+ n$  is observed at different distances from one or more reactors in a complex.

### Events (Observed/Expected) from Reactor $\bar{\nu}_e$ Experiments

VALUE	DOCUMENT ID	TECN	COMMENT
• • • We do not use the following data for averages, fits, limits, etc. • • •			
1.01 $\pm 0.024 \pm 0.053$	<sup>72</sup> BOEHM	01	Palo Verde react. 0.75–0.89 km
1.04 $\pm 0.03 \pm 0.08$	<sup>73</sup> BOEHM	00C	Palo Verde react. 0.75–0.89 km
1.01 $\pm 0.028 \pm 0.027$	<sup>74</sup> APOLLONIO	99	CHOZ Chooz reactors 1 km
0.987 $\pm 0.006 \pm 0.037$	<sup>75</sup> GREENWOOD	96	Savannah River, 18.2 m
0.988 $\pm 0.004 \pm 0.05$	ACHKAR	95	CNTR Bugey reactor, 15 m
0.994 $\pm 0.010 \pm 0.05$	ACHKAR	95	CNTR Bugey reactor, 40 m
0.915 $\pm 0.132 \pm 0.05$	ACHKAR	95	CNTR Bugey reactor, 95 m
0.987 $\pm 0.014 \pm 0.027$	<sup>76</sup> DECLAIS	94	CNTR Bugey reactor, 15 m
0.985 $\pm 0.018 \pm 0.034$	KUVSHINN...	91	CNTR Rovno reactor
1.05 $\pm 0.02 \pm 0.05$	VUILLEUMIER	82	Gösgen reactor
0.955 $\pm 0.035 \pm 0.110$	<sup>77</sup> KWON	81	$\bar{\nu}_e p \rightarrow e^+ n$
0.89 $\pm 0.15$	<sup>77</sup> BOEHM	80	$\bar{\nu}_e p \rightarrow e^+ n$
0.38 $\pm 0.21$	<sup>78,79</sup> REINES	80	
0.40 $\pm 0.22$	<sup>78,79</sup> REINES	80	

<sup>72</sup> BOEHM 01 search for neutrino oscillations at 0.75 and 0.89 km distance from the Palo Verde reactors.

<sup>73</sup> BOEHM 00C search for neutrino oscillations at 0.75 and 0.89 km distance from the Palo Verde reactors.

<sup>74</sup> APOLLONIO 99, APOLLONIO 98 search for neutrino oscillations at 1.1 km fixed distance from Chooz reactors. They use  $\bar{\nu}_e p \rightarrow e^+ n$  in Gd-loaded scintillator target. APOLLONIO 99 supersedes APOLLONIO 98.

<sup>75</sup> GREENWOOD 96 search for neutrino oscillations at 18 m and 24 m from the reactor at Savannah River.

<sup>76</sup> DECLAIS 94 result based on integral measurement of neutrons only. Result is ratio of measured cross section to that expected in standard V-A theory. Replaced by ACHKAR 95.

<sup>77</sup> KWON 81 represents an analysis of a larger set of data from the same experiment as BOEHM 80.

<sup>78</sup> REINES 80 involves comparison of neutral- and charged-current reactions  $\bar{\nu}_e d \rightarrow np\bar{\nu}_e$  and  $\bar{\nu}_e d \rightarrow nne^+$  respectively. Combined analysis of reactor  $\bar{\nu}_e$  experiments was performed by SILVERMAN 81.

<sup>79</sup> The two REINES 80 values correspond to the calculated  $\bar{\nu}_e$  fluxes of AVIGNONE 80 and DAVIS 79 respectively.

————  $\bar{\nu}_e \nrightarrow \bar{\nu}_e$  ————

### $\Delta(m^2)$ for $\sin^2(2\theta) = 1$

<u>VALUE (eV<sup>2</sup>)</u>	<u>CL%</u>	<u>DOCUMENT ID</u>	<u>TECN</u>	<u>COMMENT</u>
<b>&lt;0.0007</b>	90	80 APOLLONIO	99 CHOZ	Chooz reactors 1 km
● ● ● We do not use the following data for averages, fits, limits, etc. ● ● ●				
<0.0011	90	81 BOEHM	01	Palo Verde react. 0.75–0.89 km
<0.0011	90	82 BOEHM	00	Palo Verde react. 0.8 km
<0.01	90	83 ACHKAR	95 CNTR	Bugey reactor
<0.0075	90	84 VIDYAKIN	94	Krasnoyarsk reactors
<0.04	90	85 AFONIN	88 CNTR	Rovno reactor
<0.014	68	86 VIDYAKIN	87	$\bar{\nu}_e p \rightarrow e^+ n$
<0.019	90	87 ZACEK	86	Gösgen reactor

<sup>80</sup> APOLLONIO 99 search for neutrino oscillations at 1.1 km fixed distance from Chooz reactors. They use  $\bar{\nu}_e p \rightarrow e^+ n$  in Gd-loaded scintillator target. APOLLONIO 99 supersedes APOLLONIO 98. This is the most sensitive search in terms of  $\Delta(m^2)$  for  $\bar{\nu}_e$  disappearance.

<sup>81</sup> BOEHM 01, a continuation of BOEHM 00, is a disappearance search for neutrino oscillations at 0.75 and 0.89 km distance from the Palo Verde reactors. Result is less restrictive than APOLLONIO 99.

<sup>82</sup> BOEHM 00 is a disappearance search for neutrino oscillations at 0.75 and 0.89 km distance from Palo Verde reactors. The detection reaction is  $\bar{\nu}_e p \rightarrow e^+ n$  in a segmented Gd loaded scintillator target. Result is less restrictive than APOLLONIO 99.

<sup>83</sup> ACHKAR 95 bound is for  $L=15, 40, \text{ and } 95 \text{ m}$ .

<sup>84</sup> VIDYAKIN 94 bound is for  $L=57.0 \text{ m}, 57.6 \text{ m}, \text{ and } 231.4 \text{ m}$ . Supersedes VIDYAKIN 90.

<sup>85</sup> AFONIN 86 and AFONIN 87 also give limits on  $\sin^2(2\theta)$  for intermediate values of  $\Delta(m^2)$ . (See also KETOV 92). Supersedes AFONIN 87, AFONIN 86, AFONIN 85, AFONIN 83, and BELENKII 83.

<sup>86</sup> VIDYAKIN 87 bound is for  $L = 32.8 \text{ and } 92.3 \text{ m}$  distance from two reactors.

<sup>87</sup> This bound is from data for  $L=37.9 \text{ m}, 45.9 \text{ m}, \text{ and } 64.7 \text{ m}$ .

### $\sin^2(2\theta)$ for “Large” $\Delta(m^2)$

<u>VALUE</u>	<u>CL%</u>	<u>DOCUMENT ID</u>	<u>TECN</u>	<u>COMMENT</u>
<b>&lt;0.02</b>	90	88 ACHKAR	95 CNTR	For $\Delta(m^2) = 0.6 \text{ eV}^2$
● ● ● We do not use the following data for averages, fits, limits, etc. ● ● ●				
<0.17	90	89 BOEHM	01	Palo Verde react. 0.75–0.89 km
<0.21	90	90 BOEHM	00	Palo Verde react. 0.8 km
<0.10	90	91 APOLLONIO	99 CHOZ	Chooz reactors 1 km
<0.24	90	92 GREENWOOD	96	
<0.04	90	92 GREENWOOD	96	For $\Delta(m^2) = 1.0 \text{ eV}^2$
<0.087	68	93 VYRODOV	95 CNTR	For $\Delta(m^2) > 2 \text{ eV}^2$
<0.15	90	94 VIDYAKIN	94	For $\Delta(m^2) > 5.0 \times 10^{-2} \text{ eV}^2$
<0.2	90	95 AFONIN	88 CNTR	$\bar{\nu}_e p \rightarrow e^+ n$
<0.14	68	96 VIDYAKIN	87	$\bar{\nu}_e p \rightarrow e^+ n$
<0.21	90	97 ZACEK	86	$\bar{\nu}_e p \rightarrow e^+ n$
<0.19	90	98 ZACEK	85	Gösgen reactor
<0.16	90	99 GABATHULER	84	$\bar{\nu}_e p \rightarrow e^+ n$

- 88 ACHKAR 95 bound is from data for  $L=15, 40,$  and 95 m distance from the Bugey reactor.
- 89 BOEHM 01 search for neutrino oscillations at 0.75 and 0.89 km distance from the Palo Verde reactors. Continuation of BOEHM 00.
- 90 BOEHM 00 search for neutrino oscillations at 0.75 and 0.89 km distance from Palo Verde reactors.
- 91 APOLLONIO 99 search for neutrino oscillations at 1.1 km fixed distance from Chooz reactors.
- 92 GREENWOOD 96 search for neutrino oscillations at 18 m and 24 m from the reactor at Savannah River by observing  $\bar{\nu}_e p \rightarrow e^+ n$  in a Gd loaded scintillator target. Their region of sensitivity in  $\Delta(m^2)$  and  $\sin^2 2\theta$  is already excluded by ACHKAR 95.
- 93 The VYRODOV 95 bound is from data for  $L=15$  m distance from the Bugey-5 reactor.
- 94 The VIDYAKIN 94 bound is from data for  $L=57.0$  m, 57.6 m, and 231.4 m from three reactors in the Krasnoyarsk Reactor complex.
- 95 Several different methods of data analysis are used in AFONIN 88. We quote the most stringent limits. Different upper limits on  $\sin^2 2\theta$  apply at intermediate values of  $\Delta(m^2)$ . Supersedes AFONIN 87, AFONIN 85, and BELENKII 83.
- 96 VIDYAKIN 87 bound is for  $L = 32.8$  and 92.3 m distance from two reactors.
- 97 This bound is from data for  $L=37.9$  m, 45.9 m, and 64.7 m distance from Gosgen reactor.
- 98 ZACEK 85 gives two sets of bounds depending on what assumptions are used in the data analysis. The bounds in figure 3(a) of ZACEK 85 are progressively poorer for large  $\Delta(m^2)$  whereas those of figure 3(b) approach a constant. We list the latter. Both sets of bounds use combination of data from 37.9, 45.9, and 64.7m distance from reactor. ZACEK 85 states "Our experiment excludes this area (the oscillation parameter region allowed by the Bugey data, CAVIGNAC 84) almost completely, thus disproving the indications of neutrino oscillations of CAVIGNAC 84 with a high degree of confidence."
- 99 This bound comes from a combination of the VUILLEUMIER 82 data at distance 37.9m from Gosgen reactor and new data at 45.9m.

### (C) Atmospheric neutrino observations

Neutrinos and antineutrinos produced in the atmosphere induce  $\mu$ -like and  $e$ -like events in underground detectors. The ratio of the numbers of the two kinds of events is defined as  $\mu/e$ . It has the advantage that systematic effects, such as flux uncertainty, tend to cancel, for both experimental and theoretical values of the ratio. The "ratio of the ratios" of experimental to theoretical  $\mu/e$ ,  $R(\mu/e)$ , or that of experimental to theoretical  $\mu/\text{total}$ ,  $R(\mu/\text{total})$  with  $\text{total} = \mu + e$ , is reported below. If the actual value is not unity, the value obtained in a given experiment may depend on the experimental conditions.

**$R(\mu/e) = (\text{Measured Ratio } \mu/e) / (\text{Expected Ratio } \mu/e)$**

<u>VALUE</u>	<u>DOCUMENT ID</u>	<u>TECN</u>	<u>COMMENT</u>
• • • We do not use the following data for averages, fits, limits, etc. • • •			
$0.64 \pm 0.11 \pm 0.06$	100 ALLISON	99 SOU2	Calorimeter
$0.61 \pm 0.03 \pm 0.05$	101 FUKUDA	98 SKAM	sub-GeV
$0.66 \pm 0.06 \pm 0.08$	102 FUKUDA	98E SKAM	multi-GeV
	103 FUKUDA	96B KAMI	Water Cerenkov
$1.00 \pm 0.15 \pm 0.08$	104 DAUM	95 FREJ	Calorimeter
$0.60^{+0.06}_{-0.05} \pm 0.05$	105 FUKUDA	94 KAMI	sub-GeV
$0.57^{+0.08}_{-0.07} \pm 0.07$	106 FUKUDA	94 KAMI	multi-GeV
	107 BECKER-SZ...	92B IMB	Water Cerenkov

- 100 ALLISON 99 result is based on an exposure of 3.9 kton yr, 2.6 times the exposure reported in ALLISON 97, and replaces that result.
- 101 FUKUDA 98 result is based on an exposure of 25.5 kton yr. The analyzed data sample consists of fully-contained  $e$ -like events with  $0.1 \text{ GeV}/c < p_e$  and  $\mu$ -like events with  $0.2 \text{ GeV}/c < p_\mu$ , both having a visible energy  $< 1.33 \text{ GeV}$ . These criteria match the definition used by FUKUDA 94.
- 102 FUKUDA 98E result is based on an exposure of 25.5 kton yr. The analyzed data sample consists of fully-contained single-ring events with visible energy  $> 1.33 \text{ GeV}$  and partially contained events. All partially contained events are classified as  $\mu$ -like.
- 103 FUKUDA 96B studied neutron background in the atmospheric neutrino sample observed in the Kamiokande detector. No evidence for the background contamination was found.
- 104 DAUM 95 results are based on an exposure of 2.0 kton yr which includes the data used by BERGER 90B. This ratio is for the contained and semicontained events. DAUM 95 also report  $R(\mu/e) = 0.99 \pm 0.13 \pm 0.08$  for the total neutrino induced data sample which includes upward going stopping muons and horizontal muons in addition to the contained and semicontained events.
- 105 FUKUDA 94 result is based on an exposure of 7.7 kton yr and updates the HIRATA 92 result. The analyzed data sample consists of fully-contained  $e$ -like events with  $0.1 < p_e < 1.33 \text{ GeV}/c$  and fully-contained  $\mu$ -like events with  $0.2 < p_\mu < 1.5 \text{ GeV}/c$ .
- 106 FUKUDA 94 analyzed the data sample consisting of fully contained events with visible energy  $> 1.33 \text{ GeV}$  and partially contained  $\mu$ -like events.
- 107 BECKER-SZENDY 92B reports the fraction of nonshowering events (mostly muons from atmospheric neutrinos) as  $0.36 \pm 0.02 \pm 0.02$ , as compared with expected fraction  $0.51 \pm 0.01 \pm 0.05$ . After cutting the energy range to the Kamiokande limits, BEIER 92 finds  $R(\mu/e)$  very close to the Kamiokande value.

### $R(\nu_\mu) = (\text{Measured Flux of } \nu_\mu) / (\text{Expected Flux of } \nu_\mu)$

<u>VALUE</u>	<u>DOCUMENT ID</u>	<u>TECN</u>	<u>COMMENT</u>
● ● ● We do not use the following data for averages, fits, limits, etc. ● ● ●			
$0.72 \pm 0.026 \pm 0.13$	108 AMBROSIO	01 MCRO	upward through-going
$0.57 \pm 0.05 \pm 0.15$	109 AMBROSIO	00 MCRO	upgoing partially contained
$0.71 \pm 0.05 \pm 0.19$	110 AMBROSIO	00 MCRO	downgoing partially contained + upgoing stopping
$0.74 \pm 0.036 \pm 0.046$	111 AMBROSIO	98 MCRO	Streamer tubes
	112 CASPER	91 IMB	Water Cherenkov
	113 AGLIETTA	89 NUSX	
$0.95 \pm 0.22$	114 BOLIEV	81	Baksan
$0.62 \pm 0.17$	CROUCH	78	Case Western/UCI

- 108 AMBROSIO 01 result is based on the upward through-going muon tracks with  $E_\mu > 1 \text{ GeV}$ . The data came from three different detector configurations, but the statistics is largely dominated by the full detector run, from May 1994 to December 2000. The total live time, normalized to the full detector configuration, is 6.17 years. The first error is the statistical error, the second is the systematic error, dominated by the theoretical error in the predicted flux.
- 109 AMBROSIO 00 result is based on the upgoing partially contained event sample. It came from 4.1 live years of data taking with the full detector, from April 1994 to February 1999. The average energy of atmospheric muon neutrinos corresponding to this sample is 4 GeV. The first error is statistical, the second is the systematic error, dominated by the 25% theoretical error in the rate (20% in the flux and 15% in the cross section, added in quadrature). Within statistics, the observed deficit is uniform over the zenith angle.
- 110 AMBROSIO 00 result is based on the combined samples of downgoing partially contained events and upgoing stopping events. These two subsamples could not be distinguished due to the lack of timing information. The result came from 4.1 live years of data taking with the full detector, from April 1994 to February 1999. The average energy of atmospheric muon neutrinos corresponding to this sample is 4 GeV. The first error is

statistical, the second is the systematic error, dominated by the 25% theoretical error in the rate (20% in the flux and 15% in the cross section, added in quadrature). Within statistics, the observed deficit is uniform over the zenith angle.

- 111 AMBROSIO 98 result is for all nadir angles and updates AHLEN 95 result. The lower cutoff on the muon energy is 1 GeV. In addition to the statistical and systematic errors, there is a Monte Carlo flux error (theoretical error) of  $\pm 0.13$ . With a neutrino oscillation hypothesis, the fit either to the flux or zenith distribution independently yields  $\sin^2 2\theta = 1.0$  and  $\Delta(m^2) \sim$  a few times  $10^{-3} \text{ eV}^2$ . However, the fit to the observed zenith distribution gives a maximum probability for  $\chi^2$  of only 5% for the best oscillation hypothesis.
- 112 CASPER 91 correlates showering/nonshowering signature of single-ring events with parent atmospheric-neutrino flavor. They find nonshowering ( $\approx \nu_\mu$  induced) fraction is  $0.41 \pm 0.03 \pm 0.02$ , as compared with expected  $0.51 \pm 0.05$  (syst).
- 113 AGLIETTA 89 finds no evidence for any anomaly in the neutrino flux. They define  $\rho = (\text{measured number of } \nu_e \text{'s}) / (\text{measured number of } \nu_\mu \text{'s})$ . They report  $\rho(\text{measured}) = \rho(\text{expected}) = 0.96^{+0.32}_{-0.28}$ .
- 114 From this data BOLIEV 81 obtain the limit  $\Delta(m^2) \leq 6 \times 10^{-3} \text{ eV}^2$  for maximal mixing,  $\nu_\mu \leftrightarrow \nu_\mu$  type oscillation.

### **R( $\mu$ /total) = (Measured Ratio $\mu$ /total) / (Expected Ratio $\mu$ /total)**

<u>VALUE</u>	<u>DOCUMENT ID</u>	<u>TECN</u>	<u>COMMENT</u>
● ● ● We do not use the following data for averages, fits, limits, etc. ● ● ●			
$1.1^{+0.07}_{-0.12} \pm 0.11$	115 CLARK	97 IMB	multi-GeV

- 115 CLARK 97 obtained this result by an analysis of fully contained and partially contained events in the IMB water-Cerenkov detector with visible energy  $> 0.95 \text{ GeV}$ .

### **$N_{\text{up}}(\mu) / N_{\text{down}}(\mu)$**

<u>VALUE</u>	<u>DOCUMENT ID</u>	<u>TECN</u>	<u>COMMENT</u>
● ● ● We do not use the following data for averages, fits, limits, etc. ● ● ●			
$0.52^{+0.07}_{-0.06} \pm 0.01$	116 FUKUDA	98E SKAM	multi-GeV

- 116 FUKUDA 98E result is based on an exposure of 25.5 kton yr. The analyzed data sample consists of fully-contained single-ring  $\mu$ -like events with visible energy  $> 1.33 \text{ GeV}$  and partially contained events. All partially contained events are classified as  $\mu$ -like. Upward-going events are those with  $-1 < \cos(\text{zenith angle}) < -0.2$  and downward-going events with those with  $0.2 < \cos(\text{zenith angle}) < 1$ . FUKUDA 98E result strongly deviates from an expected value of  $0.98 \pm 0.03 \pm 0.02$ .

### **$N_{\text{up}}(e) / N_{\text{down}}(e)$**

<u>VALUE</u>	<u>DOCUMENT ID</u>	<u>TECN</u>	<u>COMMENT</u>
● ● ● We do not use the following data for averages, fits, limits, etc. ● ● ●			
$0.84^{+0.14}_{-0.12} \pm 0.02$	117 FUKUDA	98E SKAM	multi-GeV

- 117 FUKUDA 98E result is based on an exposure of 25.5 kton yr. The analyzed data sample consists of fully-contained single-ring  $e$ -like events with visible energy  $> 1.33 \text{ GeV}$ . Upward-going events are those with  $-1 < \cos(\text{zenith angle}) < -0.2$  and downward-going events are those with  $0.2 < \cos(\text{zenith angle}) < 1$ . FUKUDA 98E result is compared to an expected value of  $1.01 \pm 0.06 \pm 0.03$ .

### $\sin^2(2\theta)$ for given $\Delta(m^2)$ ( $\nu_e \leftrightarrow \nu_\mu$ )

For a review see BAHCALL 89.

<u>VALUE</u>	<u>CL%</u>	<u>DOCUMENT ID</u>	<u>TECN</u>	<u>COMMENT</u>
● ● ● We do not use the following data for averages, fits, limits, etc. ● ● ●				
<0.6	90	118 OYAMA	98 KAMI	$\Delta(m^2) > 0.1 \text{ eV}^2$
<0.5		119 CLARK	97 IMB	$\Delta(m^2) > 0.1 \text{ eV}^2$
>0.55	90	120 FUKUDA	94 KAMI	$\Delta(m^2) = 0.007\text{--}0.08 \text{ eV}^2$
<0.47	90	121 BERGER	90B FREJ	$\Delta(m^2) > 1 \text{ eV}^2$
<0.14	90	LOSECCO	87 IMB	$\Delta(m^2) = 0.00011 \text{ eV}^2$

118 OYAMA 98 obtained this result by an analysis of upward-going muons in Kamiokande. The data sample used is essentially the same as that used by HATAKEYAMA 98.

119 CLARK 97 obtained this result by an analysis of fully contained and partially contained events in the IMB water-Cerenkov detector with visible energy  $> 0.95 \text{ GeV}$ .

120 FUKUDA 94 obtained this result by a combined analysis of sub- and multi-GeV atmospheric neutrino events in Kamiokande.

121 BERGER 90B uses the Frejus detector to search for oscillations of atmospheric neutrinos. Bounds are for both neutrino and antineutrino oscillations.

### $\Delta(m^2)$ for $\sin^2(2\theta) = 1$ ( $\nu_e \leftrightarrow \nu_\mu$ )

<u>VALUE (<math>10^{-5} \text{ eV}^2</math>)</u>	<u>CL%</u>	<u>DOCUMENT ID</u>	<u>TECN</u>
--	------------	--------------------	-------------

● ● ● We do not use the following data for averages, fits, limits, etc. ● ● ●

<560	90	122 OYAMA	98 KAMI
<980		123 CLARK	97 IMB
$700 < \Delta(m^2) < 7000$	90	124 FUKUDA	94 KAMI
<150	90	125 BERGER	90B FREJ

122 OYAMA 98 obtained this result by an analysis of upward-going muons in Kamiokande. The data sample used is essentially the same as that used by HATAKEYAMA 98.

123 CLARK 97 obtained this result by an analysis of fully contained and partially contained events in the IMB water-Cerenkov detector with visible energy  $> 0.95 \text{ GeV}$ .

124 FUKUDA 94 obtained this result by a combined analysis of sub- and multi-GeV atmospheric neutrino events in Kamiokande.

125 BERGER 90B uses the Frejus detector to search for oscillations of atmospheric neutrinos. Bounds are for both neutrino and antineutrino oscillations.

### $\sin^2(2\theta)$ for given $\Delta(m^2)$ ( $\bar{\nu}_e \leftrightarrow \bar{\nu}_\mu$ )

<u>VALUE (<math>10^{-5} \text{ eV}^2</math>)</u>	<u>CL%</u>	<u>DOCUMENT ID</u>	<u>TECN</u>	<u>COMMENT</u>
--	------------	--------------------	-------------	----------------

● ● ● We do not use the following data for averages, fits, limits, etc. ● ● ●

<0.9	99	126 SMIRNOV	94 THEO	$\Delta(m^2) > 3 \times 10^{-4} \text{ eV}^2$
<0.7	99	126 SMIRNOV	94 THEO	$\Delta(m^2) < 10^{-11} \text{ eV}^2$

126 SMIRNOV 94 analyzed the data from SN 1987A using stellar-collapse models. They also give less stringent upper limits on  $\sin^2 2\theta$  for  $10^{-11} < \Delta(m^2) < 3 \times 10^{-7} \text{ eV}^2$  and  $10^{-5} < \Delta(m^2) < 3 \times 10^{-4} \text{ eV}^2$ . The same results apply to  $\bar{\nu}_e \leftrightarrow \bar{\nu}_\tau$ ,  $\nu_\mu$ , and  $\nu_\tau$ .



**$\sin^2(2\theta)$  for given  $\Delta(m^2)$  ( $\nu_\mu \leftrightarrow \nu_\tau$ )**

<u>VALUE</u>	<u>CL%</u>	<u>DOCUMENT ID</u>	<u>TECN</u>	<u>COMMENT</u>
• • •				We do not use the following data for averages, fits, limits, etc. • • •
>0.8	90	127 AMBROSIO	01 MCRO	$\Delta(m^2)= 0.0006\text{--}0.015 \text{ eV}^2$
>0.82	90	128 AMBROSIO	01 MCRO	$\Delta(m^2)= 0.001\text{--}0.006 \text{ eV}^2$
>0.25	90	129 AMBROSIO	00 MCRO	$\Delta(m^2) > 3 \times 10^{-4} \text{ eV}^2$
>0.4	90	130 FUKUDA	99C SKAM	$\Delta(m^2)= 0.001\text{--}0.1 \text{ eV}^2$
>0.7	90	131 FUKUDA	99D SKAM	$\Delta(m^2)= 0.0015\text{--}0.015 \text{ eV}^2$
>0.82	90	132 AMBROSIO	98 MCRO	$\Delta(m^2) \sim 0.0025 \text{ eV}^2$
>0.82	90	133 FUKUDA	98C SKAM	$\Delta(m^2) = 0.0005\text{--}0.006 \text{ eV}^2$
>0.3	90	134 HATAKEYAMA	98 KAMI	$\Delta(m^2)= 0.00055\text{--}0.14 \text{ eV}^2$
>0.73	90	135 HATAKEYAMA	98 KAMI	$\Delta(m^2)= 0.004\text{--}0.025 \text{ eV}^2$
<0.7		136 CLARK	97 IMB	$\Delta(m^2) > 0.1 \text{ eV}^2$
>0.65	90	137 FUKUDA	94 KAMI	$\Delta(m^2) = 0.005\text{--}0.03 \text{ eV}^2$
<0.5	90	138 BECKER-SZ...	92 IMB	$\Delta(m^2)= 1\text{--}2 \times 10^{-4} \text{ eV}^2$
<0.6	90	139 BERGER	90B FREJ	$\Delta(m^2) > 1 \text{ eV}^2$

127 AMBROSIO 01 result is based on the angular distribution of upward through-going muon tracks with  $E_\mu > 1 \text{ GeV}$ . The data came from three different detector configurations, but the statistics is largely dominated by the full detector run, from May 1994 to December 2000. The total live time, normalized to the full detector configuration, is 6.17 years. The best fit is obtained outside the physical region. The method of FELDMAN 98 is used to obtain the limits.

128 AMBROSIO 01 result is based on the angular distribution and normalization of upward through-going muon tracks with  $E_\mu > 1 \text{ GeV}$ . The best fit is obtained outside the physical region. The method of FELDMAN 98 is used to obtain the limits. See the previous footnote.

129 AMBROSIO 00 obtained this result by using the upgoing partially contained event sample and the combined samples of downgoing partially contained events and upgoing stopping events. These data came from 4.1 live years of data taking with the full detector, from April 1994 to February 1999. The average energy of atmospheric muon neutrinos corresponding to these samples is 4 GeV. The maximum of the  $\chi^2$  probability (97%) occurs at maximal mixing and  $\Delta(m^2)=(1\sim 20) \times 10^{-3} \text{ eV}^2$ .

130 FUKUDA 99C obtained this result from a total of 537 live days of upward through-going muon data in Super-Kamiokande between April 1996 to January 1998. With a threshold of  $E_\mu > 1.6 \text{ GeV}$ , the observed flux of upward through-going muons is  $(1.74 \pm 0.07 \pm 0.02) \times 10^{-13} \text{ cm}^{-2} \text{ s}^{-1} \text{ sr}^{-1}$ . The zenith-angle dependence of the flux does not agree with no-oscillation predictions. For the  $\nu_\mu \rightarrow \nu_\tau$  hypothesis, FUKUDA 99C obtained the best fit at  $\sin^2 2\theta=0.95$  and  $\Delta(m^2)=5.9 \times 10^{-3} \text{ eV}^2$ . FUKUDA 99C also reports 68% and 99% confidence-level allowed regions for the same hypothesis.

131 FUKUDA 99D obtained this result from a simultaneous fitting to zenith angle distributions of upward-stopping and through-going muons. The flux of upward-stopping muons of minimum energy of 1.6 GeV measured between April 1996 and January 1998 is  $(0.39 \pm 0.04 \pm 0.02) \times 10^{-13} \text{ cm}^{-2} \text{ s}^{-1} \text{ sr}^{-1}$ . This is compared to the expected flux of  $(0.73 \pm 0.16 \text{ (theoretical error)}) \times 10^{-13} \text{ cm}^{-2} \text{ s}^{-1} \text{ sr}^{-1}$ . The flux of upward through-going muons is taken from FUKUDA 99C. For the  $\nu_\mu \rightarrow \nu_\tau$  hypothesis, FUKUDA 99D obtained the best fit in the physical region at  $\sin^2 2\theta=1.0$  and  $\Delta(m^2)=3.9 \times 10^{-3} \text{ eV}^2$ . FUKUDA 99D also reports 68% and 99% confidence-level allowed regions for the same hypothesis. FUKUDA 99D further reports the result of the oscillation analysis using the zenith-angle dependence of upward-stopping/through-going flux ratio. The best fit in the physical region is obtained at  $\sin^2 2\theta=1.0$  and  $\Delta(m^2)=3.1 \times 10^{-3} \text{ eV}^2$ .

- 132 AMBROSIO 98 result is only 17% probable at maximum because of relatively low flux for  $\cos\theta < -0.8$ .
- 133 FUKUDA 98C obtained this result by an analysis of 33.0 kton yr atmospheric-neutrino data which include the 25.5 kton yr data used by FUKUDA 98 (sub-GeV) and FUKUDA 98E (multi-GeV). Inside the physical region, the best fit was obtained at  $\sin^2 2\theta=1.0$  and  $\Delta(m^2)=2.2 \times 10^{-3} \text{ eV}^2$ . In addition, FUKUDA 98C gave the 99% confidence interval,  $\sin^2 2\theta > 0.73$  and  $3 \times 10^{-4} < \Delta(m^2) < 8.5 \times 10^{-3} \text{ eV}^2$ . FUKUDA 98C also tested the  $\nu_\mu \rightarrow \nu_e$  hypothesis, and concluded that it is not favored.
- 134 HATAKEYAMA 98 obtained this result from a total of 2456 live days of upward-going muon data in Kamiokande between December 1985 and May 1995. With a threshold of  $E_\mu > 1.6 \text{ GeV}$ , the observed flux of upward through-going muon is  $(1.94 \pm 0.10_{-0.06}^{+0.07}) \times 10^{-13} \text{ cm}^{-2} \text{ s}^{-1} \text{ sr}^{-1}$ . This is compared to the expected flux of  $(2.46 \pm 0.54 \text{ (theoretical error)}) \times 10^{-13} \text{ cm}^{-2} \text{ s}^{-1} \text{ sr}^{-1}$ . For the  $\nu_\mu \rightarrow \nu_\tau$  hypothesis, the best fit inside the physical region was obtained at  $\sin^2 2\theta=1.0$  and  $\Delta(m^2)=3.2 \times 10^{-3} \text{ eV}^2$ .
- 135 HATAKEYAMA 98 obtained this result from a combined analysis of Kamiokande's contained events (FUKUDA 94) and upward-going muon events. The best fit was obtained at  $\sin^2 2\theta=0.95$  and  $\Delta(m^2)=1.3 \times 10^{-2} \text{ eV}^2$ .
- 136 CLARK 97 obtained this result by an analysis of fully contained and partially contained events in the IMB water-Cerenkov detector with visible energy  $> 0.95 \text{ GeV}$ .
- 137 FUKUDA 94 obtained this result by a combined analysis of sub-and multi-GeV atmospheric neutrino events in Kamiokande.
- 138 BECKER-SZENDY 92 uses upward-going muons to search for atmospheric  $\nu_\mu$  oscillations. The fraction of muons which stop in the detector is used to search for deviations in the expected spectrum. No evidence for oscillations is found.
- 139 BERGER 90B uses the Frejus detector to search for oscillations of atmospheric neutrinos. Bounds are for both neutrino and antineutrino oscillations.

### $\Delta(m^2)$ for $\sin^2(2\theta) = 1$ ( $\nu_\mu \leftrightarrow \nu_\tau$ )

VALUE ( $10^{-5} \text{ eV}^2$ )	CL%	DOCUMENT ID	TECN
----------------------------------	-----	-------------	------

• • • We do not use the following data for averages, fits, limits, etc. • • •

$60 < \Delta(m^2) < 1500$	90	140 AMBROSIO	01 MCRO
$100 < \Delta(m^2) < 600$	90	141 AMBROSIO	01 MCRO
$> 35$	90	142 AMBROSIO	00 MCRO
$100 < \Delta(m^2) < 5000$	90	143 FUKUDA	99C SKAM
$150 < \Delta(m^2) < 1500$	90	144 FUKUDA	99D SKAM
$50 < \Delta(m^2) < 600$	90	145 AMBROSIO	98 MCRO
$50 < \Delta(m^2) < 600$	90	146 FUKUDA	98C SKAM
$55 < \Delta(m^2) < 5000$	90	147 HATAKEYAMA98	KAMI
$400 < \Delta(m^2) < 2300$	90	148 HATAKEYAMA98	KAMI
$< 1500$		149 CLARK	97 IMB
$500 < \Delta(m^2) < 2500$	90	150 FUKUDA	94 KAMI
$< 350$	90	151 BERGER	90B FREJ

- 140 AMBROSIO 01 result is based on the angular distribution of upward through-going muon tracks with  $E_\mu > 1 \text{ GeV}$ . The data came from three different detector configurations, but the statistics is largely dominated by the full detector run, from May 1994 to December 2000. The total live time, normalized to the full detector configuration, is 6.17 years. The best fit is obtained outside the physical region. The method of FELDMAN 98 is used to obtain the limits.

- 141 AMBROSIO 01 result is based on the angular distribution and normalization of upward through-going muon tracks with  $E_\mu > 1$  GeV. The best fit is obtained outside the physical region. The method of FELDMAN 98 is used to obtain the limits. See the previous footnote.
- 142 AMBROSIO 00 obtained this result by using the upgoing partially contained event sample and the combined samples of downgoing partially contained events and upgoing stopping events. These data came from 4.1 live years of data taking with the full detector, from April 1994 to February 1999. The average energy of atmospheric muon neutrinos corresponding to these samples is 4 GeV. The maximum of the  $\chi^2$  probability (97%) occurs at maximal mixing and  $\Delta(m^2)=(1\sim 20) \times 10^{-3} \text{ eV}^2$ .
- 143 FUKUDA 99C obtained this result from a total of 537 live days of upward through-going muon data in Super-Kamiokande between April 1996 to January 1998. With a threshold of  $E_\mu > 1.6$  GeV, the observed flux of upward through-going muon is  $(1.74 \pm 0.07 \pm 0.02) \times 10^{-13} \text{ cm}^{-2} \text{ s}^{-1} \text{ sr}^{-1}$ . The zenith-angle dependence of the flux does not agree with no-oscillation predictions. For the  $\nu_\mu \rightarrow \nu_\tau$  hypothesis, FUKUDA 99C obtained the best fit at  $\sin^2 2\theta=0.95$  and  $\Delta(m^2)=5.9 \times 10^{-3} \text{ eV}^2$ . FUKUDA 99C also reports 68% and 99% confidence-level allowed regions for the same hypothesis.
- 144 FUKUDA 99D obtained this result from a simultaneous fitting to zenith angle distributions of upward-stopping and through-going muons. The flux of upward-stopping muons of minimum energy of 1.6 GeV measured between April 1996 and January 1998 is  $(0.39 \pm 0.04 \pm 0.02) \times 10^{-13} \text{ cm}^{-2} \text{ s}^{-1} \text{ sr}^{-1}$ . This is compared to the expected flux of  $(0.73 \pm 0.16 \text{ (theoretical error)}) \times 10^{-13} \text{ cm}^{-2} \text{ s}^{-1} \text{ sr}^{-1}$ . The flux of upward through-going muons is taken from FUKUDA 99C. For the  $\nu_\mu \rightarrow \nu_\tau$  hypothesis, FUKUDA 99D obtained the best fit in the physical region at  $\sin^2 2\theta=1.0$  and  $\Delta(m^2)=3.9 \times 10^{-3} \text{ eV}^2$ . FUKUDA 99D also reports 68% and 99% confidence-level allowed regions for the same hypothesis. FUKUDA 99D further reports the result of the oscillation analysis using the zenith-angle dependence of upward-stopping/through-going flux ratio. The best fit in the physical region is obtained at  $\sin^2 2\theta=1.0$  and  $\Delta(m^2)=3.1 \times 10^{-3} \text{ eV}^2$ .
- 145 AMBROSIO 98 result is only 17% probable at maximum because of relatively low flux for  $\cos\theta < -0.8$ .
- 146 FUKUDA 98C obtained this result by an analysis of 33.0 kton yr atmospheric-neutrino data which include the 25.5 kton yr data used by FUKUDA 98 (sub-GeV) and FUKUDA 98E (multi-GeV). Inside the physical region, the best fit was obtained at  $\sin^2 2\theta=1.0$  and  $\Delta(m^2)=2.2 \times 10^{-3} \text{ eV}^2$ . In addition, FUKUDA 98C gave the 99% confidence interval,  $\sin^2 2\theta > 0.73$  and  $3 \times 10^{-4} < \Delta(m^2) < 8.5 \times 10^{-3} \text{ eV}^2$ . FUKUDA 98C also tested the  $\nu_\mu \rightarrow \nu_e$  hypothesis, and concluded that it is not favored.
- 147 HATAKEYAMA 98 obtained this result from a total of 2456 live days of upward-going muon data in Kamiokande between December 1985 and May 1995. With a threshold of  $E_\mu > 1.6$  GeV, the observed flux of upward through-going muon is  $(1.94 \pm 0.10^{+0.07}_{-0.06}) \times 10^{-13} \text{ cm}^{-2} \text{ s}^{-1} \text{ sr}^{-1}$ . This is compared to the expected flux of  $(2.46 \pm 0.54 \text{ (theoretical error)}) \times 10^{-13} \text{ cm}^{-2} \text{ s}^{-1} \text{ sr}^{-1}$ . For the  $\nu_\mu \rightarrow \nu_\tau$  hypothesis, the best fit inside the physical region was obtained at  $\sin^2 2\theta=1.0$  and  $\Delta(m^2)=3.2 \times 10^{-3} \text{ eV}^2$ .
- 148 HATAKEYAMA 98 obtained this result from a combined analysis of Kamiokande's contained events (FUKUDA 94) and upward-going muon events. The best fit was obtained at  $\sin^2 2\theta=0.95$  and  $\Delta(m^2)=1.3 \times 10^{-2} \text{ eV}^2$ .
- 149 CLARK 97 obtained this result by an analysis of fully contained and partially contained events in the IMB water-Cerenkov detector with visible energy  $> 0.95$  GeV.
- 150 FUKUDA 94 obtained this result by a combined analysis of sub-and multi-GeV atmospheric neutrino events in Kamiokande.
- 151 BERGER 90B uses the Frejus detector to search for oscillations of atmospheric neutrinos. Bounds are for both neutrino and antineutrino oscillations.

## $\Delta(m^2)$ for $\sin^2(2\theta) = 1$ ( $\nu_\mu \rightarrow \nu_s$ )

$\nu_s$  means  $\nu_\tau$  or any sterile (noninteracting)  $\nu$ .

VALUE ( $10^{-5}$ eV <sup>2</sup> )	CL%	DOCUMENT ID	TECN	COMMENT
-------------------------------------	-----	-------------	------	---------

• • • We do not use the following data for averages, fits, limits, etc. • • •

<3000 (or <550)	90	<sup>152</sup> OYAMA	89	KAMI Water Cerenkov
< 4.2 or > 54.	90	BIONTA	88	IMB Flux has $\nu_\mu, \bar{\nu}_\mu, \nu_e,$ and $\bar{\nu}_e$

<sup>152</sup>OYAMA 89 gives a range of limits, depending on assumptions in their analysis. They argue that the region  $\Delta(m^2) = (100-1000) \times 10^{-5}$  eV<sup>2</sup> is not ruled out by any data for large mixing.

## Search for $\nu_\mu \rightarrow \nu_s$

VALUE	DOCUMENT ID	TECN	COMMENT
-------	-------------	------	---------

• • • We do not use the following data for averages, fits, limits, etc. • • •

<sup>153</sup> AMBROSIO	01	MCRO	matter effects
<sup>154</sup> FUKUDA	00	SKAM	neutral currents + matter effects

<sup>153</sup>AMBROSIO 01 tested the pure 2-flavor  $\nu_\mu \rightarrow \nu_s$  hypothesis using matter effects which change the shape of the zenith-angle distribution of upward through-going muons. With maximum mixing and  $\Delta(m^2)$  around 0.0024 eV<sup>2</sup>, the  $\nu_\mu \rightarrow \nu_s$  oscillation is disfavored with 99% confidence level with respect to the  $\nu_\mu \rightarrow \nu_\tau$  hypothesis.

<sup>154</sup>FUKUDA 00 tested the pure 2-flavor  $\nu_\mu \rightarrow \nu_s$  hypothesis using three complementary atmospheric-neutrino data samples. With this hypothesis, zenith-angle distributions are expected to show characteristic behavior due to neutral currents and matter effects. In the  $\Delta(m^2)$  and  $\sin^2 2\theta$  region preferred by the Super-Kamiokande data, the  $\nu_\mu \rightarrow \nu_s$  hypothesis is rejected at the 99% confidence level, while the  $\nu_\mu \rightarrow \nu_\tau$  hypothesis consistently fits all of the data sample.

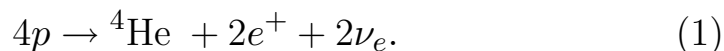
## (D) Solar $\nu$ Experiments

### SOLAR NEUTRINOS

Revised April 2002 by K. Nakamura (KEK, High Energy Accelerator Research Organization, Japan).

#### 1. Introduction

The Sun is a main-sequence star at a stage of stable hydrogen burning. It produces an intense flux of electron neutrinos as a consequence of nuclear fusion reactions whose combined effect is



Positrons annihilate with electrons. Therefore, when considering the solar thermal energy generation, a relevant expression is

$$4p + 2e^- \rightarrow {}^4\text{He} + 2\nu_e + 26.73 \text{ MeV} - E_\nu, \quad (2)$$

where  $E_\nu$  represents the energy taken away by neutrinos, with an average value being  $\langle E_\nu \rangle \sim 0.6 \text{ MeV}$ . The neutrino-producing reactions which are at work inside the Sun are enumerated in the first column in Table 1. The second column in Table 1 shows abbreviation of these reactions. The energy spectrum of each reaction is shown in Fig. 1.

A pioneering solar neutrino experiment by Davis and collaborators using  ${}^{37}\text{Cl}$  started in the late 1960's. Since then, chlorine and gallium radiochemical experiments and water Čerenkov experiments with light and heavy water targets have made successful solar-neutrino observations.

Observation of solar neutrinos directly addresses the theory of stellar structure and evolution, which is the basis of the standard solar model (SSM). The Sun as a well-defined neutrino source also provides extremely important opportunities to investigate nontrivial neutrino properties such as nonzero mass and mixing, because of the wide range of matter density and the very long distance from the Sun to the Earth.

From the very beginning of the solar-neutrino observation, it was recognized that the observed flux was significantly smaller than the SSM prediction provided nothing happens to the electron neutrinos after they are created in the solar interior. This deficit has been called “the solar-neutrino problem.” The initial result from Sudbury Neutrino Observatory (SNO) on the solar neutrino flux measured via charged-current reaction  $\nu_e d \rightarrow e^- pp$ , combined with the Super-Kamiokande's high-statistics flux measurement via  $\nu_e e$  elastic scattering, provided

**Table 1:** Neutrino-producing reactions in the Sun (the first column) and their abbreviations (second column). The neutrino fluxes and event rates in chlorine and gallium solar-neutrino experiments predicted by Bahcall, Pinsonneault, and Basu [1] are listed in the third, fourth, and fifth columns respectively.

Reaction	Abbr.	BP2000 [1]		
		Flux ( $\text{cm}^{-2} \text{s}^{-1}$ )	Cl (SNU*)	Ga (SNU*)
$pp \rightarrow d e^+ \nu$	$pp$	$5.95(1.00^{+0.01}_{-0.01}) \times 10^{10}$	—	69.7
$pe^- p \rightarrow d \nu$	$pep$	$1.40(1.00^{+0.015}_{-0.015}) \times 10^8$	0.22	2.8
${}^3\text{He } p \rightarrow {}^4\text{He } e^+ \nu$	$hep$	$9.3 \times 10^3$	0.04	0.1
${}^7\text{Be } e^- \rightarrow {}^7\text{Li } \nu + (\gamma)$	${}^7\text{Be}$	$4.77(1.00^{+0.10}_{-0.10}) \times 10^9$	1.15	34.2
${}^8\text{B} \rightarrow {}^8\text{Be}^* e^+ \nu$	${}^8\text{B}$	$5.05(1.00^{+0.20}_{-0.16}) \times 10^6$	5.76	12.1
${}^{13}\text{N} \rightarrow {}^{13}\text{C } e^+ \nu$	${}^{13}\text{N}$	$5.48(1.00^{+0.21}_{-0.17}) \times 10^8$	0.09	3.4
${}^{15}\text{O} \rightarrow {}^{15}\text{N } e^+ \nu$	${}^{15}\text{O}$	$4.80(1.00^{+0.25}_{-0.19}) \times 10^8$	0.33	5.5
${}^{17}\text{F} \rightarrow {}^{17}\text{O } e^+ \nu$	${}^{17}\text{F}$	$5.63(1.00^{+0.25}_{-0.25}) \times 10^6$	0.0	0.1
Total			$7.6^{+1.3}_{-1.1}$	$128^{+9}_{-7}$

\* 1 SNU (Solar Neutrino Unit) =  $10^{-36}$  captures per atom per second.

direct evidence for flavor conversion of solar neutrinos. The most probable explanation is neutrino oscillation which can also solve the solar-neutrino problem. The recent SNO's result of the neutral-current measurement,  $\nu d \rightarrow \nu pn$ , and the updated charged-current result further strengthened this conclusion.

## 2. Solar Model Predictions

A standard solar model is based on the standard theory of stellar evolution. A variety of input information is needed in the evolutionary calculations. The most elaborate SSM, BP2000 [1], is presented by Bahcall *et al.* who define their SSM as the solar model which is constructed with the best available physics and input data. Though they used no helioseismological constraints in defining the SSM, the calculated sound speed as a function of

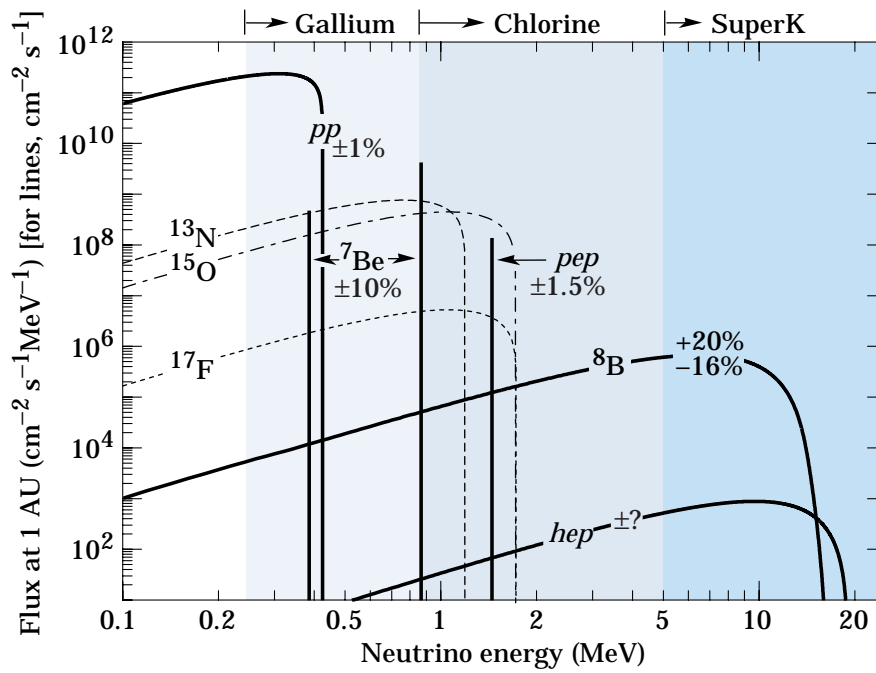


**Figure 1:** The solar neutrino spectrum predicted by the standard solar model. The neutrino fluxes from continuum sources are given in units of number  $\text{cm}^{-2}\text{s}^{-1}\text{MeV}^{-1}$  at one astronomical unit, and the line fluxes are given in number  $\text{cm}^{-2}\text{s}^{-1}$ . Spectra for the  $pp$  chain, shown by the solid curves, are courtesy of J.N. Bahcall (2001). Spectra for the CNO chain are shown by the dotted curves, and are also courtesy of J.N. Bahcall (1995).

the solar radius shows an excellent agreement with the helioseismologically determined sound speed to a precision of 0.1% rms throughout essentially the entire Sun. This greatly strengthens confidence in the solar model. The BP2000 prediction [1] for the flux, contributions to the event rates in chlorine and gallium solar-neutrino experiments from each neutrino-producing

reaction is listed in Table 1. The solar-neutrino spectra shown in Fig. 1 also resulted from the BP2000 calculations [1].

Another recent solar-model predictions for solar-neutrino fluxes were given by Turck-Chieze *et al.* [2] Their model is based on the standard theory of stellar evolution where the best

physics available is adopted, but some fundamental inputs such as the  $p$ - $p$  reaction rate and the heavy-element abundance in the Sun are seismically adjusted within the commonly estimated errors aiming at reducing the residual differences between the helioseismologically-determined and the model-calculated sound speeds. Their predictions for the event rates in chlorine and gallium solar-neutrino experiments as well as  $^8\text{B}$  solar-neutrino flux are shown in the last line in Table 2, where the BP2000 predictions [1] are also shown in the same format. As is apparent from this table, the predictions of the two models are remarkably consistent.

The SSM predicted  $^8\text{B}$  solar-neutrino flux is proportional to the low-energy cross section factor  $S_{17}(0)$  for the  $^7\text{Be}(p,\gamma)^8\text{B}$  reaction. The BP2000 [1] and Turck-Chieze *et al.* [2] models adopted  $S_{17}(0) = 19_{-2}^{+4}$  eV·b. Inspired by the recent precise measurement of the low-energy cross section for the  $^7\text{Be}(p,\gamma)^8\text{B}$  reaction by Junghans *et al.* [3], Bahcall *et al.* [4] calculated the (BP2000 + New  $^8\text{B}$ ) SSM predictions using  $S_{17}(0) = (22.3 \pm 0.9)$  eV·b. The results are: the  $^8\text{B}$  solar-neutrino flux of  $5.93(1.00_{-0.15}^{+0.14}) \times 10^6$  cm $^{-2}$  s $^{-1}$ , the chlorine capture rate of  $8.59_{-1.2}^{+1.1}$  SNU, and the gallium capture rate of  $130_{-7}^{+9}$  SNU.

### ***3. Solar Neutrino Experiments***

So far, seven solar-neutrino experiments have published results. The most recent published results on the average event



**Table 2:** Recent results from the seven solar-neutrino experiments and a comparison with standard solar-model predictions. Solar model calculations are also presented. The first and the second errors in the experimental results are the statistical and systematic errors, respectively.

	$^{37}\text{Cl}\rightarrow^{37}\text{Ar}$ (SNU)	$^{71}\text{Ga}\rightarrow^{71}\text{Ge}$ (SNU)	$^8\text{B } \nu$ flux ( $10^6\text{cm}^{-2}\text{s}^{-1}$ )
Homestake			
(CLEVELAND 98)[5]	$2.56 \pm 0.16 \pm 0.16$	—	—
GALLEX			
(HAMPEL 99)[6]	—	$77.5 \pm 6.2^{+4.3}_{-4.7}$	—
GNO			
(ALTMANN 00)[7]	—	$65.8^{+10.2+3.4}_{-9.6-3.6}$	—
SAGE			
(ABDURASHI...99B)[8]	—	$67.2^{+7.2+3.5}_{-7.0-3.0}$	—
Kamiokande			
(FUKUDA 96)[9]	—	—	$2.80 \pm 0.19 \pm 0.33^\dagger$
Super-Kamiokande			
(FUKUDA 01)[10]	—	—	$2.32 \pm 0.03^{+0.08^\dagger}_{-0.07}$
SNO			
(AHMAD 02)[11]	—	—	$1.76^{+0.06}_{-0.05} \pm 0.09^\ddagger$
	—	—	$2.39^{+0.24}_{-0.23} \pm 0.12^\dagger$
	—	—	$5.09^{+0.44+0.46*}_{-0.43-0.43}$
(BAHCALL 01)[1]	$7.6^{+1.3}_{-1.1}$	$128^{+9}_{-7}$	$5.05(1.00^{+0.20}_{-0.16})$
(TURCK-CHIEZE 01)[2]	$7.44 \pm 0.96$	$127.8 \pm 8.6$	$4.95 \pm 0.72$

\* Flux measured via the neutral-current reaction.

† Flux measured via  $\nu e$  elastic scattering.

‡ Flux measured via the charged-current reaction.

rates or flux from these experiments are listed in Table 2 and compared to the two recent solar-model predictions.

### 3.1. Radiochemical Experiments

Radiochemical experiments exploit electron neutrino absorption on nuclei followed by their decay through orbital electron capture. Produced Auger electrons are counted.

The Homestake chlorine experiment in USA uses the reaction



Three gallium experiments (GALLEX and GNO at Gran Sasso in Italy and SAGE at Baksan in Russia) use the reaction



The produced  ${}^{37}\text{Ar}$  and  ${}^{71}\text{Ge}$  atoms are both radioactive, with half lives ( $\tau_{1/2}$ ) of 34.8 days and 11.43 days, respectively. After an exposure of the detector for two to three times  $\tau_{1/2}$ , the reaction products are chemically extracted and introduced into a low-background proportional counter, and are counted for a sufficiently long period to determine the exponentially decaying signal and a constant background.

Solar-model calculations predict that the dominant contribution in the chlorine experiment comes from  ${}^8\text{B}$  neutrinos, but  ${}^7\text{Be}$ ,  $pp$ ,  ${}^{13}\text{N}$ , and  ${}^{15}\text{O}$  neutrinos also contribute. At present, the most abundant  $pp$  neutrinos can be detected only in gallium experiments. Even so, according to the solar-model calculations almost half of the capture rate in the gallium experiments is due to other solar neutrinos.

The Homestake chlorine experiment was the first attempt to observe solar neutrinos. Initial results obtained in 1968 showed no events above background with upper limit of the solar-neutrino flux of 3 SNU [13]. After introduction of an improved electronics system which discriminates signal from background by measuring the rise time of the pulses from proportional

counters, finite solar-neutrino flux has been observed since 1970. The solar-neutrino capture rate shown in Table 2 is a combined result of 108 runs between 1970 and 1994 [5]. It is only about 1/3 of the BP2000 prediction [1].

GALLEX presented the first evidence of  $pp$  solar-neutrino observation in 1992 [14]. Here also, the observed capture rate is significantly less than the SSM prediction. SAGE initially reported very low capture rate,  $20_{-20}^{+15} \pm 32$  SNU, with a 90% confidence-level upper limit of 79 SNU [15]. Later, SAGE observed similar capture rate to that of GALLEX [16]. Both GALLEX and SAGE groups tested the overall detector response with intense man-made  $^{51}\text{Cr}$  neutrino sources, and observed good agreement between the measured  $^{71}\text{Ge}$  production rate and that predicted from the source activity, demonstrating the reliability of these experiments. The GALLEX Collaboration formally finished observations in early 1997. Since April, 1998, a newly defined collaboration, GNO (Gallium Neutrino Observatory) resumed the observations.

### ***3.2 Kamiokande and Super-Kamiokande***

Kamiokande and Super-Kamiokande in Japan are real-time experiments utilizing  $\nu e$  scattering

$$\nu_x + e^- \rightarrow \nu_x + e^- \quad (5)$$

in a large water-Čerenkov detector. It should be noted that the reaction Eq. (5) is sensitive to all active neutrinos,  $x = e, \mu,$  and  $\tau$ . However, the sensitivity to  $\nu_\mu$  and  $\nu_\tau$  is much smaller than the sensitivity to  $\nu_e$ ,  $\sigma(\nu_{\mu,\tau}e) \approx 0.16 \sigma(\nu_e e)$ . The solar-neutrino flux measured via  $\nu e$  scattering is deduced assuming no neutrino oscillations.

These experiments take advantage of the directional correlation between the incoming neutrino and the recoil electron. This

feature greatly helps the clear separation of the solar-neutrino signal from the background. Due to the high thresholds (7 MeV in Kamiokande and 5 MeV at present in Super-Kamiokande) the experiments observe pure  ${}^8\text{B}$  solar neutrinos because *hep* neutrinos contribute negligibly according to the SSM.

The Kamiokande-II Collaboration started observing the  ${}^8\text{B}$  solar neutrinos at the beginning of 1987. Because of the strong directional correlation of  $\nu e$  scattering, this result gave the first direct evidence that the Sun emits neutrinos [17] (no directional information is available in radiochemical solar-neutrino experiments). The observed solar-neutrino flux was also significantly less than the SSM prediction. In addition, Kamiokande-II obtained the energy spectrum of recoil electrons and the fluxes separately measured in the daytime and nighttime. The Kamiokande-II experiment came to an end at the beginning of 1995.

Super-Kamiokande is a 50-kton second-generation solar-neutrino detector, which is characterized by a significantly larger counting rate than the first-generation experiments. This experiment started observation in April 1996. The average solar-neutrino flux is smaller than, but consistent with, the Kamiokande-II result. The flux measured in the nighttime is slightly higher than the flux measured in the daytime, but it is only a  $1.3\sigma$  effect [10]. Super-Kamiokande also observed the recoil-electron energy spectrum. Initially, its shape showed an excess at the high-energy end ( $> 13$  MeV) compared to the SSM expectation, though its statistical significance was not very high [18]. More recent results indicate that the high-energy excess is reduced with the accumulation of statistics and it is concluded that the recoil electron spectrum is consistent with no spectral distortion [10].

### 3.3 SNO

In 1999, a new realtime solar-neutrino experiment, SNO (Sudbury Neutrino Observatory) in Canada started observation. This experiment uses 1000 tons of ultra-pure heavy water (D<sub>2</sub>O) contained in a spherical acrylic vessel, surrounded by ultra-pure H<sub>2</sub>O shield. SNO measures <sup>8</sup>B solar neutrinos via the reactions

$$\nu_e + d \rightarrow e^- + p + p \quad (6)$$

and

$$\nu_x + d \rightarrow \nu_x + p + n, \quad (7)$$

as well as  $\nu e$  scattering, Eq. (5). The charged-current (CC) reaction, Eq. (6), is sensitive only to electron neutrinos, while the neutral-current (NC) reaction, Eq. (7), is sensitive to all active neutrinos.

The Q-value of the CC reaction is  $-1.4$  MeV and the electron energy is strongly correlated with the neutrino energy. Thus, the CC reaction provides an accurate measure of the shape of the <sup>8</sup>B solar-neutrino spectrum. The contributions from the CC reaction and  $\nu e$  scattering can be distinguished by using different  $\cos \theta_\odot$  distributions where  $\theta_\odot$  is the angle with respect to the direction from the Sun to the Earth. While the  $\nu e$  scattering events have a strong forward peak, CC events have an approximate angular distribution of  $1 - 1/3 \cos \theta_\odot$ .

The threshold of the NC reaction is 2.2 MeV. In the pure D<sub>2</sub>O, the signal of the NC reaction is neutron capture in deuterium, producing a 6.25-MeV  $\gamma$ -ray. In this case, capture efficiency is low and the deposited energy is close to the detection threshold of 5 MeV. In order to enhance both the capture efficiency and the total  $\gamma$ -ray energy (8.6 MeV), 2.5 tons of NaCl has been added to the heavy water in the second phase of the experiment. In addition, installation of discrete

$^3\text{He}$  neutron counters is planned for the NC measurement in the third phase.

In 2001, the SNO Collaboration published the initial results on the measurement of the  $^8\text{B}$  solar-neutrino flux via CC reaction [12]. The electron energy spectrum and the  $\cos\theta_\odot$  distribution have also been measured. The spectral shape of the electron energy is consistent with the expectations for no oscillation.

SNO also measured the  $^8\text{B}$  solar-neutrino flux via  $\nu e$  scattering. Though the latter result has poor statistics yet, it is consistent with the high-statistics Super-Kamiokande result. Thus, the SNO group compared their CC result with Super-Kamiokande's  $\nu e$  scattering result, and obtained evidence of an active non- $\nu_e$  component in the solar-neutrino flux, as further described in Sec. 3.5.

More recently, in April, 2002, the SNO Collaboration reported the first result on the  $^8\text{B}$  solar-neutrino flux measurement via NC reaction [11]. The total flux measured via NC reaction is consistent with the solar-model predictions (see Table 2).

Also, the SNO's CC and  $\nu e$  scattering results were updated [11]. These results are consistent with the earlier results [12].

### ***3.4 Comparison of Experimental Results with Solar-Model Predictions***

It is clear from Table 2 that the results from all the solar-neutrino experiments, except the most recent SNO NC result, indicate significantly less flux than expected from the BP2000 SSM [1] and the Turck-Chieze *et al.* solar model [2].

There has been a consensus that a consistent explanation of all the results of solar-neutrino observations is unlikely within the framework of astrophysics using the solar-neutrino

spectra given by the standard electroweak model. Many authors made solar model-independent analyses constrained by the observed solar luminosity [19–23], where they attempted to fit the measured solar-neutrino capture rates and  $^8\text{B}$  flux with normalization-free, undistorted energy spectra. All these attempts only obtained solutions with very low probabilities.

The data therefore suggest that the solution to the solar-neutrino problem requires nontrivial neutrino properties.

### ***3.5 Evidence for Solar Neutrino Oscillations***

Denoting the  $^8\text{B}$  solar-neutrino flux obtained by the SNO CC measurement as  $\phi_{\text{SNO}}^{\text{CC}}(\nu_e)$  and that obtained by the Super-Kamiokande  $\nu e$  scattering as  $\phi_{\text{SK}}^{\text{ES}}(\nu_x)$ ,  $\phi_{\text{SNO}}^{\text{CC}}(\nu_e) = \phi_{\text{SK}}^{\text{ES}}(\nu_x)$  is expected for the standard neutrino physics. However, SNO's initial data [12] indicate

$$\phi_{\text{SK}}^{\text{ES}}(\nu_x) - \phi_{\text{SNO}}^{\text{CC}}(\nu_e) = (0.57 \pm 0.17) \times 10^6 \text{ cm}^{-2}\text{s}^{-1}. \quad (8)$$

The significance of the difference is  $> 3\sigma$ , implying direct evidence for the existence of a non- $\nu_e$  active neutrino flavor component in the solar-neutrino flux. A natural and most probable explanation of neutrino flavor conversion is neutrino oscillation. Note that both the SNO [12] and Super-Kamiokande [10] flux results were obtained by assuming the standard  $^8\text{B}$  neutrino spectrum shape. This assumption is justified by the measured energy spectra in both of the experiments.

From the measured  $\phi_{\text{SNO}}^{\text{CC}}(\nu_e)$  and  $\phi_{\text{SK}}^{\text{ES}}(\nu_x)$ , the flux of non- $\nu_e$  active neutrinos,  $\phi(\nu_\mu \text{ or } \tau)$ , and the total flux of active  $^8\text{B}$  solar neutrinos,  $\phi(\nu_x)$ , can be deduced [12]:

$$\phi(\nu_\mu \text{ or } \tau) = (3.69 \pm 1.13) \times 10^6 \text{ cm}^{-2}\text{s}^{-1} \quad (9)$$

and

$$\phi(\nu_x) = (5.44 \pm 0.99) \times 10^6 \text{ cm}^{-2}\text{s}^{-1}. \quad (10)$$

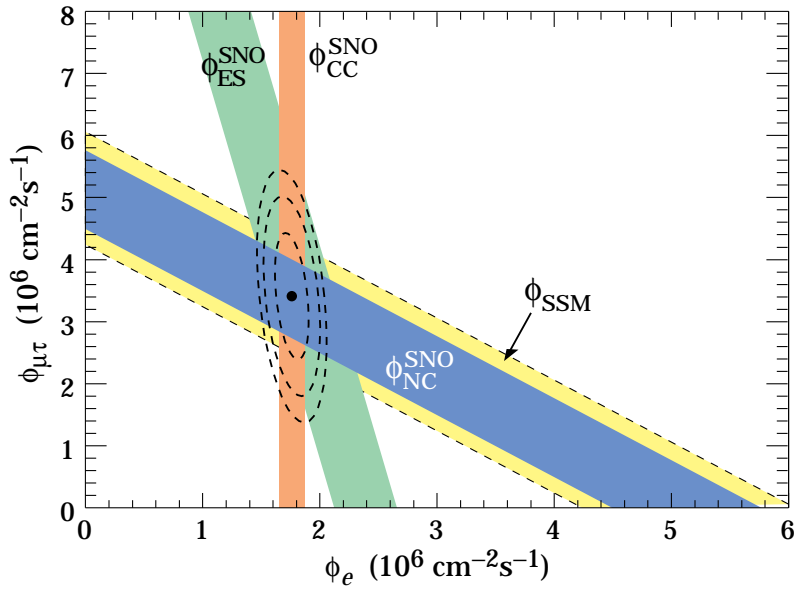


**Figure 2:** Fluxes of  ${}^8\text{B}$  solar neutrinos,  $\phi(\nu_e)$ , and  $\phi(\nu_\mu \text{ or } \tau)$ , deduced from the SNO's charged-current (CC),  $\nu_e$  elastic scattering (ES), and neutral-current (NC) results. The standard solar model prediction [1] is also shown. The bands represent the  $1\sigma$  error. The contours show the 68%, 90%, and 97% joint probability for  $\phi(\nu_e)$  and  $\phi(\nu_\mu \text{ or } \tau)$ . This figure is courtesy of K.T. Lesko (LBNL).

Eq. (10) is a solar model-independent result and therefore tests solar models. It shows very good agreement with the  ${}^8\text{B}$  solar-neutrino flux predicted by the BP2000 SSM [1] and that predicted by Turck-Chieze *et al.* model [2].

The recently reported SNO's results [11] are

$$\phi_{\text{SNO}}^{\text{CC}}(\nu_e) = (1.76_{-0.05}^{+0.06} \pm 0.09) \times 10^6 \text{ cm}^{-2} \text{ s}^{-1}, \quad (11)$$



$$\phi_{\text{SNO}}^{\text{ES}}(\nu_x) = (2.39_{-0.23}^{+0.24} \pm 0.12) \times 10^6 \text{cm}^{-2} \text{s}^{-1}, \quad (12)$$

$$\phi_{\text{SNO}}^{\text{NC}}(\nu_x) = (5.09_{-0.43-0.43}^{+0.44+0.46}) \times 10^6 \text{cm}^{-2} \text{s}^{-1}. \quad (13)$$

The fluxes  $\phi(\nu_e)$  and  $\phi(\nu_\mu \text{ or } \tau)$  deduced from these results are remarkably consistent as can be seen in Fig. 2. The resultant  $\phi(\nu_\mu \text{ or } \tau)$  is

$$\phi(\nu_\mu \text{ or } \tau) = (3.41_{-0.64}^{+0.66}) \times 10^6 \text{cm}^{-2} \text{s}^{-1} \quad (14)$$

where the statistical and systematic errors are added in quadrature. Now  $\phi(\nu_\mu \text{ or } \tau)$  is  $5.3 \sigma$  above 0, providing stronger evidence for neutrino oscillation than Eq. (8).

#### 4. *Global Analyses of the Solar Neutrino Data*

A number of pre-SNO global analyses of the solar-neutrino data in terms of two neutrino oscillations yielded various solutions. For example, Bahcall, Krastev, and Smirnov [24] found at 99.7% confidence level eight allowed discrete regions in two-neutrino oscillation space. These are five solutions for active neutrinos (LMA, SMA, LOW, VAC, and Just So<sup>2</sup>) and three separate solutions for sterile neutrinos (SMA(sterile), VAC(sterile), and Just So<sup>2</sup>(sterile)). LMA, SMA, LOW, VAC are abbreviations of large mixing angle, small mixing angle, low probability or low mass, and vacuum, respectively. The best-fit points for the five solutions for active neutrinos are shown below.

- LMA:  $\Delta m^2 = 4.2 \times 10^{-5} \text{ eV}^2$ ,  $\tan^2 \theta = 0.26$
- SMA:  $\Delta m^2 = 5.2 \times 10^{-6} \text{ eV}^2$ ,  $\tan^2 \theta = 5.5 \times 10^{-4}$
- LOW:  $\Delta m^2 = 7.6 \times 10^{-8} \text{ eV}^2$ ,  $\tan^2 \theta = 0.72$
- Just So<sup>2</sup>:  $\Delta m^2 = 5.5 \times 10^{-12} \text{ eV}^2$ ,  $\tan^2 \theta = 1.0$
- VAC:  $\Delta m^2 = 1.4 \times 10^{-10} \text{ eV}^2$ ,  $\tan^2 \theta = 0.38$ .

For the three solutions for sterile neutrinos, the best-fit points are similar to the corresponding solutions for active neutrinos.

Immediately after the report of SNO's first result [12], many authors [25–28] presented the results of global analyses including the SNO's CC data. In most of these analyses, the total event rates from chlorine and gallium experiments, SNO's CC event rate, and Super-Kamiokande's day and night spectra are used. The total event rate from Super-Kamiokande is not used because it is not independent from the spectral data. The theoretical solar-neutrino fluxes are taken from BP2000 SSM [1].

A common feature of the analyses which include Super-Kamiokande's spectral data [10] are:

- The LMA solution is most favored.
- The LOW and VAC solutions are next or thirdly favored depending on the analysis detail.
- The SMA solution is a significantly less good solution than the LOW and VAC solutions.
- All other solutions generally give poor fits except that the VAC(sterile) solution sometimes gives as good a fit as the VAC or LOW solution.

It should be noted that all the favored solutions, LMA, LOW, and VAC, have large mixing angles.

### ***5. Future Prospects***

The SNO solar-neutrino measurement established solar-neutrino oscillations at  $> 5\sigma$  level. The next step is to determine the solution uniquely. The forthcoming data from SNO and from new solar-neutrino experiments will provide important clues to discriminate the solutions.

Future SNO results will include the day-night flux asymmetry, more precise energy spectrum, and NC/CC ratio. SNO's expected day-night effect is substantially larger at the best-fit region of the LMA solution than at the best-fit region of the

LOW solution. However, for both the LMA and LOW solutions, no spectrum distortion is expected. The SMA and VAC solutions will give detectable spectrum distortion. Very recently SNO announced a possible day-night asymmetry of  $\phi(\nu_e)$ , which favors the LMA solution [29].

An important task of the future solar neutrino experiments is the measurement of monochromatic  ${}^7\text{Be}$  solar neutrinos. If the VAC solution is correct, the flux of  ${}^7\text{Be}$  neutrinos shows larger seasonal variations than the flux of  ${}^8\text{B}$  neutrinos. In the LOW region, a strong day-night effect is expected. The  ${}^7\text{Be}$  neutrino flux will be measured by a new experiment, Borexino, at Gran Sasso *via*  $\nu e$  scattering in 300 tons of ultra-pure liquid scintillator with a detection threshold as low as 250 keV. The Borexino experiment is expected to turn on in 2002.

KamLAND is an experiment similar to, but larger than Borexino. It is located at Kamioka, and 1000 tons of ultra-pure liquid scintillator is used. This experiment will also observe  ${}^7\text{Be}$  neutrinos if the detection threshold can be lowered to a level similar to that of Borexino. However, one of the primary purposes of this experiment is the observation of oscillations of neutrinos produced by power reactors. The sensitivity region of KamLAND includes the LMA solution. Thus, the presently most-favored LMA solution may be proved or excluded by KamLAND. KamLAND is expected to turn on early in 2002.

## References

1. J.N. Bahcall, M.H. Pinsonneault, and S. Basu, *Astrophys. J.* **555**, 990 (2001).
2. S. Turck-Chieze *et al.*, *Astrophys. J.* **555**, L69 (2001).
3. A.R. Junghans *et al.*, *Phys. Rev. Lett.* **88**, 041101 (2002).
4. J.N. Bahcall, M.C. Gonzalez-Garcia, and C. Pena-Garay, *JHEP* **0204**, 007 (2002).

5. B.T. Cleveland *et al.*, Ap. J. **496**, 505 (1998).
6. W. Hampel *et al.*, Phys. Lett. **B447**, 127 (1999).
7. M. Altmann *et al.*, Phys. Lett. **B490**, 16 (2000).
8. J.N. Abdurashitov *et al.*, Phys. Rev. **C60**, 0055801 (1999).
9. Y. Fukuda *et al.*, Phys. Rev. Lett. **77**, 1683 (1996).
10. Y. Fukuda *et al.*, Phys. Rev. Lett. **86**, 5651 (2001).
11. Q.R. Ahmad *et al.*, `nucl-ex/0204008`.
12. Q.R. Ahmad *et al.*, Phys. Rev. Lett. **87**, 071301 (2001).
13. R. Davis, Jr. *et al.*, Phys. Rev. Lett. **20**, 1205 (1968).
14. P. Anselmann *et al.*, Phys. Lett. **B285**, 376 (1994).
15. A.I. Abazov *et al.*, Phys. Rev. Lett. **67**, 3332 (1991).
16. J.N. Abdurashitov *et al.*, Phys. Lett. **B328**, 234 (1994).
17. K.S. Hirata *et al.*, Phys. Rev. Lett. **63**, 16 (1989).
18. Y. Fukuda *et al.*, Phys. Rev. Lett. **82**, 2430 (1999).
19. N. Hata, S. Bludman, and P. Langacker, Phys. Rev. **D49**, 3622 (1994).
20. N. Hata and P. Langacker, Phys. Rev. **D52**, 420 (1995).
21. N. Hata and P. Langacker, Phys. Rev. **D56**, 6107 (1997).
22. S. Parke, Phys. Rev. Lett. **74**, 839 (1995).
23. K.M. Heeger and R.G.H. Robertson, Phys. Rev. Lett. **77**, 3720 (1996).
24. J.N. Bahcall, P.I. Krastev, and A.Yu. Smirnov, JHEP 05, 015 (2001).
25. G.L. Fogli *et al.*, Phys. Rev. **D64**, 093007 (2001).
26. J.N. Bahcall, M.C. Gonzalez-Garcia, and C. Pena-Garay, JHEP 08, 014 (2001).
27. A. Bandyopadhyay *et al.*, Phys. Lett. **B519**, 83 (2001).
28. P.I. Krastev and A. Yu. Smirnov, Phys. Rev. **D65**, 073022 (2002).
29. Q.R. Ahmad *et al.*, `nucl-ex/0204009`.

## $\nu_e$ Capture Rates from Radiochemical Experiments

1 SNU (Solar Neutrino Unit) =  $10^{-36}$  captures per atom per second.

VALUE (SNU)	DOCUMENT ID	TECN	COMMENT
65.8 $\begin{smallmatrix} +10.2 & +3.4 \\ -9.6 & -3.6 \end{smallmatrix}$	155 ALTMANN	00 GNO	$^{71}\text{Ga} \rightarrow ^{71}\text{Ge}$
74.1 $\begin{smallmatrix} +6.7 \\ -6.8 \end{smallmatrix}$	156 ALTMANN	00 GNO	GNO + GALX combined
67.2 $\begin{smallmatrix} +7.2 & +3.5 \\ -7.0 & -3.0 \end{smallmatrix}$	157 ABDURASHI...	99B SAGE	$^{71}\text{Ga} \rightarrow ^{71}\text{Ge}$
77.5 $\begin{smallmatrix} \pm 6.2 & +4.3 \\ & -4.7 \end{smallmatrix}$	158 HAMPEL	99 GALX	$^{71}\text{Ga} \rightarrow ^{71}\text{Ge}$
2.56 $\pm 0.16 \pm 0.16$	159 CLEVELAND	98 HOME	$^{37}\text{Cl} \rightarrow ^{37}\text{Ar}$

155 ALTMANN 00 report the first result from the GNO solar-neutrino experiment (GNO I), which is the successor project of GALLEX. Experimental technique of GNO is essentially the same as that of GALLEX. The run data cover the period 20 May 1998 through 12 January 2000.

156 Combined result of GALLEX I+II+III+IV (HAMPEL 99) and GNO I. The indicated errors include systematic errors.

157 ABDURASHITOV 99B is a detailed report of the SAGE solar-neutrino experiment during the period January 1990 through December 1997, and updates the ABDURASHITOV 94 result. However the data in the period November 1993 through June 1994 were not used in determining the neutrino capture rate due to some uncertainty with respect to experimental control. A total of 211  $^{71}\text{Ge}$  events were observed.

158 HAMPEL 99 report the combined result for GALLEX I+II+III+IV (65 runs in total), which update the HAMPEL 96 result. The GALLEX IV result (12 runs) is  $118.4 \pm 17.8 \pm 6.6$  SNU. (HAMPEL 99 discuss the consistency of partial results with the mean.) The GALLEX experimental program has been completed with these runs. The total run data cover the period 14 May 1991 through 23 January 1997. A total of 300  $^{71}\text{Ge}$  events were observed.

159 CLEVELAND 98 is a detailed report of the  $^{37}\text{Cl}$  experiment at the Homestake Mine. The average solar neutrino-induced  $^{37}\text{Ar}$  production rate from 108 runs between 1970 and 1994 updates the DAVIS 89 result.

## $\phi_{ES} (^8\text{B})$

$^8\text{B}$  solar-neutrino flux measured via  $\nu_e$  elastic scattering. This process is sensitive to all active neutrino flavors, but with reduced sensitivity to  $\nu_\mu, \nu_\tau$  due to the cross-section difference,  $\sigma(\nu_{\mu,\tau} e) \sim 0.16\sigma(\nu_e e)$ . If the  $^8\text{B}$  solar-neutrino flux involves nonelectron flavor active neutrinos, their contribution to the flux is  $\sim 0.16$  times of  $\nu_e$ .

VALUE ( $10^6 \text{ cm}^{-2}\text{s}^{-1}$ )	DOCUMENT ID	TECN	COMMENT
<b>2.33 <math>\begin{smallmatrix} +0.08 \\ -0.07 \end{smallmatrix}</math> OUR AVERAGE</b>			
2.39 $\begin{smallmatrix} +0.24 \\ -0.23 \end{smallmatrix} \pm 0.12$	160 AHMAD	02 SNO	average flux
2.32 $\pm 0.03 \begin{smallmatrix} +0.08 \\ -0.07 \end{smallmatrix}$	161 FUKUDA	01 SKAM	average flux

• • • We do not use the following data for averages, fits, limits, etc. • • •

$2.39 \pm 0.34 \begin{smallmatrix} +0.16 \\ -0.14 \end{smallmatrix}$	162 AHMAD	01	SNO	average flux
$2.28 \pm 0.04 \begin{smallmatrix} +0.08 \\ -0.07 \end{smallmatrix}$	161 FUKUDA	01	SKAM	day flux
$2.36 \pm 0.04 \begin{smallmatrix} +0.08 \\ -0.07 \end{smallmatrix}$	161 FUKUDA	01	SKAM	night flux
$2.80 \pm 0.19 \pm 0.33$	163 FUKUDA	96	KAMI	average flux
$2.70 \pm 0.27$	163 FUKUDA	96	KAMI	day flux
$2.87 \begin{smallmatrix} +0.27 \\ -0.26 \end{smallmatrix}$	163 FUKUDA	96	KAMI	night flux

160 AHMAD 02 reports the  $^8\text{B}$  solar-neutrino flux measured via  $\nu e$  elastic scattering above the kinetic energy threshold of 5 MeV. The data correspond to 306.4 live days with SNO between November 2, 1999 and May 28, 2001, and updates AHMAD 01 results.

161 FUKUDA 01 results are for 1258 live days with Super-Kamiokande between May 31, 1996 and October 6, 2000, and replace FUKUDA 99 results. The analysis threshold is 5 MeV except for the first 280 live days (6.5 MeV).

162 AHMAD 01 reports the  $^8\text{B}$  solar-neutrino flux measured via  $\nu e$  elastic scattering above the kinetic energy threshold of 6.75 MeV. The data correspond to 241 live days with SNO between November 2, 1999 and January 15, 2001.

163 FUKUDA 96 results are for a total of 2079 live days with Kamiokande II and III from January 1987 through February 1995, covering the entire solar cycle 22, with threshold  $E_e > 9.3$  MeV (first 449 days),  $> 7.5$  MeV (middle 794 days), and  $> 7.0$  MeV (last 836 days). These results update the HIRATA 90 result for the average  $^8\text{B}$  solar-neutrino flux and HIRATA 91 result for the day-night variation in the  $^8\text{B}$  solar-neutrino flux. The total data sample was also analyzed for short-term variations: within experimental errors, no strong correlation of the solar-neutrino flux with the sunspot numbers was found.

### $\phi_{CC} (^8\text{B})$

$^8\text{B}$  solar-neutrino flux measured with charged-current reaction which is sensitive exclusively to  $\nu_e$ .

<u>VALUE (<math>10^6 \text{ cm}^{-2}\text{s}^{-1}</math>)</u>	<u>DOCUMENT ID</u>	<u>TECN</u>	<u>COMMENT</u>
$1.76 \begin{smallmatrix} +0.06 \\ -0.05 \end{smallmatrix} \pm 0.09$	164 AHMAD	02	SNO average flux

• • • We do not use the following data for averages, fits, limits, etc. • • •

$1.75 \pm 0.07 \begin{smallmatrix} +0.12 \\ -0.11 \end{smallmatrix} \pm 0.05$	165 AHMAD	01	SNO average flux
---	-----------	----	------------------

164 AHMAD 02 reports the SNO result of the  $^8\text{B}$  solar-neutrino flux measured with charged-current reaction on deuterium,  $\nu_e d \rightarrow ppe^-$ , above the kinetic energy threshold of 5 MeV. The data correspond to 306.4 live days with SNO between November 2, 1999 and May 28, 2001, and updates AHMAD 01 results.

165 AHMAD 01 reports the first SNO result of the  $^8\text{B}$  solar-neutrino flux measured with the charged-current reaction on deuterium,  $\nu_e d \rightarrow ppe^-$ , above the kinetic energy threshold of 6.75 MeV. The data correspond to 241 live days with SNO between November 2, 1999 and January 15, 2001.

### $\phi_{NC} (^8\text{B})$

$^8\text{B}$  solar neutrino flux measured with neutral-current reaction, which is equally sensitive to  $\nu_e$ ,  $\nu_\mu$ , and  $\nu_\tau$ .

<u>VALUE (<math>10^6 \text{ cm}^{-2}\text{s}^{-1}</math>)</u>	<u>DOCUMENT ID</u>	<u>TECN</u>	<u>COMMENT</u>
$5.09 \begin{smallmatrix} +0.44 +0.46 \\ -0.43 -0.43 \end{smallmatrix}$	166 AHMAD	02	SNO average flux

<sup>166</sup> AHMAD 02 reports the first SNO result of the <sup>8</sup>B solar-neutrino flux measured with the neutral-current reaction on deuterium,  $\nu_\ell d \rightarrow n p \nu_\ell$ , above the neutral-current reaction threshold of 2.2 MeV. The data correspond to 306.4 live days with SNO between November 2, 1999 and May 28, 2001.

### $\phi_{\nu_\mu + \nu_\tau}$ (<sup>8</sup>B)

Nonelectron-flavor active neutrino component ( $\nu_\mu$  and  $\nu_\tau$ ) in the <sup>8</sup>B solar-neutrino flux.

VALUE ( $10^6 \text{ cm}^{-2}\text{s}^{-1}$ )	DOCUMENT ID	TECN	COMMENT
$3.41 \pm 0.45^{+0.48}_{-0.45}$	<sup>167</sup> AHMAD	02 SNO	Derived from SNO $\phi_{CC}$ , $\phi_{ES}$ , and $\phi_{NC}$

• • • We do not use the following data for averages, fits, limits, etc. • • •

$3.69 \pm 1.13$	<sup>168</sup> AHMAD	01	Derived from SNO+SuperKam, water Cherenkov
-----------------	----------------------	----	--

<sup>167</sup> AHMAD 02 deduced the nonelectron-flavor active neutrino component ( $\nu_\mu$  and  $\nu_\tau$ ) in the <sup>8</sup>B solar-neutrino flux, by combining the charged-current result, the  $\nu e$  elastic-scattering result and the neutral-current result.

<sup>168</sup> AHMAD 01 deduced the nonelectron-flavor active neutrino component ( $\nu_\mu$  and  $\nu_\tau$ ) in the <sup>8</sup>B solar-neutrino flux, by combining the SNO charged-current result (AHMAD 01) and the Super-Kamiokande  $\nu e$  elastic-scattering result (FUKUDA 01).

### Total Flux of Active <sup>8</sup>B Solar Neutrinos

Total flux of active neutrinos ( $\nu_e$ ,  $\nu_\mu$ , and  $\nu_\tau$ ).

VALUE ( $10^6 \text{ cm}^{-2}\text{s}^{-1}$ )	DOCUMENT ID	TECN	COMMENT
$5.09^{+0.44+0.46}_{-0.43-0.43}$	<sup>169</sup> AHMAD	02 SNO	Direct measurement from $\phi_{NC}$
$5.44 \pm 0.99$	<sup>170</sup> AHMAD	01	Derived from SNO+SuperKam, water Cherenkov

<sup>169</sup> AHMAD 02 determined the total flux of active <sup>8</sup>B solar neutrinos by directly measuring the neutral-current reaction,  $\nu_\ell d \rightarrow n p \nu_\ell$ , which is equally sensitive to  $\nu_e$ ,  $\nu_\mu$ , and  $\nu_\tau$ .

<sup>170</sup> AHMAD 01 deduced the total flux of active <sup>8</sup>B solar neutrinos by combining the SNO charged-current result (AHMAD 01) and the Super-Kamiokande  $\nu e$  elastic-scattering result (FUKUDA 01).

### Day-Night Asymmetry (<sup>8</sup>B)

$$A = (\phi_{\text{night}} - \phi_{\text{day}}) / \phi_{\text{average}}$$

VALUE	DOCUMENT ID	TECN	COMMENT
$0.14 \pm 0.063^{+0.015}_{-0.014}$	<sup>171</sup> AHMAD	02B SNO	Derived from SNO $\phi_{CC}$
$0.07 \pm 0.049^{+0.013}_{-0.012}$	<sup>172</sup> AHMAD	02B SNO	Constraint of no $\phi_{NC}$ asymmetry
$0.033 \pm 0.022^{+0.013}_{-0.012}$	<sup>173</sup> FUKUDA	01 SKAM	Based on $\phi_{ES}$

- 171 AHMAD 02B results are based on the charged-current interactions recorded between November 2, 1999 and May 28, 2001, with the day and night live times of 128.5 and 177.9 days, respectively.
- 172 AHMAD 02B results are derived from the charged-current interactions, neutral-current interactions, and  $\nu e$  elastic scattering, with the total flux of active neutrinos constrained to have no asymmetry. The data were recorded between November 2, 1999 and May 28, 2001, with the day and night live times of 128.5 and 177.9 days, respectively.
- 173 FUKUDA 01 results are for 1258 live days with the Super-Kamiokande between May 31, 1996 and October 6, 2000, and replace FUKUDA 99 results. The analysis threshold is 5 MeV except for the first 280 live days (6.5 MeV).

### $\phi_{ES}$ (hep)

hep solar-neutrino flux measured via  $\nu e$  elastic scattering. This process is sensitive to all active neutrino flavors, but with reduced sensitivity to  $\nu_\mu, \nu_\tau$  due to the cross-section difference,  $\sigma(\nu_{\mu,\tau} e) \sim 0.16\sigma(\nu_e e)$ . If the hep solar-neutrino flux involves nonelectron flavor active neutrinos, their contribution to the flux is  $\sim 0.16$  times of  $\nu_e$ .

VALUE ( $10^3 \text{ cm}^{-2}\text{s}^{-1}$ )	CL%	DOCUMENT ID	TECN
<40	90	174 FUKUDA	01 SKAM

- 174 FUKUDA 01 result is obtained from the recoil electron energy window of 18–21 MeV, and the obtained 90% confidence level upper limit is 4.3 times the BP2000 Standard-Solar-Model prediction.

## REFERENCES FOR Neutrino Mixing

AHMAD 02	nucl-ex/0204008	Q.R. Ahmad <i>et al.</i>	(SNO Collab.)
PRL (to be publ.)			
AHMAD 02B	nucl-ex/0204009	Q.R. Ahmad <i>et al.</i>	(SNO Collab.)
PRL (to be publ.)			
AGUILAR 01	PR D64 112007	A. Aguilar <i>et al.</i>	(LSND Collab.)
AHMAD 01	PRL 87 071301	Q.R. Ahmad <i>et al.</i>	(SNO Collab.)
AMBROSIO 01	PL B517 59	M. Ambrosio <i>et al.</i>	(MACRO Collab.)
ASTIER 01B	NP B611 3	P. Astier <i>et al.</i>	(NOMAD Collab.)
BOEHM 01	PR D64 112001	F. Boehm <i>et al.</i>	
ESKUT 01	PL B497 8	E. Eskut <i>et al.</i>	(CHORUS Collab.)
FUKUDA 01	PRL 86 5651	S. Fukuda <i>et al.</i>	(Super-Kamiokande Collab.)
ALTMANN 00	PL B490 16	M. Altmann <i>et al.</i>	(GNO Collab.)
AMBROSIO 00	PL B478 5	M. Ambrosio <i>et al.</i>	(MACRO Collab.)
BOEHM 00	PRL 84 3764	F. Boehm <i>et al.</i>	
BOEHM 00C	PR D62 072002	F. Boehm <i>et al.</i>	
FUKUDA 00	PRL 85 3999	S. Fukuda <i>et al.</i>	(Super-Kamiokande Collab.)
ABDURASHI... 99B	PR C60 055801	J.N. Abdurashitov <i>et al.</i>	(SAGE Collab.)
ALLISON 99	PL B449 137	W.W.M. Allison <i>et al.</i>	(Soudan 2 Collab.)
APOLLONIO 99	PL B466 415	M. Apollonio <i>et al.</i>	(CHOOZ Collab.)
Also 00	PL B472 434 erratum	M. Apollonio <i>et al.</i>	(CHOOZ Collab.)
FUKUDA 99	PRL 82 1810	Y. Fukuda <i>et al.</i>	(Super-Kamiokande Collab.)
FUKUDA 99C	PRL 82 2644	Y. Fukuda <i>et al.</i>	(Super-Kamiokande Collab.)
FUKUDA 99D	PL B467 185	Y. Fukuda <i>et al.</i>	(Super-Kamiokande Collab.)
HAMPEL 99	PL B447 127	W. Hampel <i>et al.</i>	(GALLEX Collab.)
JUNK 99	NIM A434 435	T. Junk	
NAPLES 99	PR D59 031101	D. Naples <i>et al.</i>	(CCFR Collab.)
ALTEGOER 98B	PL B431 219	S. Altegoer <i>et al.</i>	(NOMAD Collab.)
AMBROSIO 98	PL B434 451	M. Ambrosio <i>et al.</i>	(MACRO Collab.)
APOLLONIO 98	PL B420 397	M. Apollonio <i>et al.</i>	(CHOOZ Collab.)
ARMBRUSTER 98	PR C57 3414	B. Armbruster <i>et al.</i>	(KARMEN Collab.)
ATHANASSO... 98	PRL 81 1774	C. Athanassopoulos <i>et al.</i>	(LSND Collab.)
ATHANASSO... 98B	PR C58 2489	C. Athanassopoulos <i>et al.</i>	(LSND Collab.)
CLEVELAND 98	APJ 496 505	B.T. Cleveland <i>et al.</i>	(Homestake Collab.)
ESKUT 98	PL B424 202	E. Eskut <i>et al.</i>	(CHORUS Collab.)
ESKUT 98B	PL B434 205	E. Eskut <i>et al.</i>	(CHORUS Collab.)



FELDMAN	98	PR D57 3873	G.J. Feldman, R.D. Cousins	
FUKUDA	98	PL B433 9	Y. Fukuda <i>et al.</i>	(Super-Kamiokande Collab.)
FUKUDA	98C	PRL 81 1562	Y. Fukuda <i>et al.</i>	(Super-Kamiokande Collab.)
FUKUDA	98E	PL B436 33	Y. Fukuda <i>et al.</i>	(Super-Kamiokande Collab.)
HAMPEL	98	PL B420 114	W. Hampel <i>et al.</i>	(GALLEX Collab.)
HATAKEYAMA	98	PRL 81 2016	S. Hatakeyama <i>et al.</i>	(Kamiokande Collab.)
OYAMA	98	PR D57 R6594	Y. Oyama	
ALLISON	97	PL B391 491	W.W.M. Allison <i>et al.</i>	(Soudan 2 Collab.)
CLARK	97	PRL 79 345	R. Clark <i>et al.</i>	(IMB Collab.)
ROMOSAN	97	PRL 78 2912	A. Romosan <i>et al.</i>	(CCFR Collab.)
ATHANASSO...	96	PR C54 2685	C. Athanassopoulos <i>et al.</i>	(LSND Collab.)
ATHANASSO...	96B	PRL 77 3082	C. Athanassopoulos <i>et al.</i>	(LSND Collab.)
BORISOV	96	PL B369 39	A.A. Borisov <i>et al.</i>	(SERP, JINR)
FUKUDA	96	PRL 77 1683	Y. Fukuda <i>et al.</i>	(Kamiokande Collab.)
FUKUDA	96B	PL B388 397	Y. Fukuda <i>et al.</i>	(Kamiokande Collab.)
GREENWOOD	96	PR D53 6054	Z.D. Greenwood <i>et al.</i>	(UCI, SVR, SCUC)
HAMPEL	96	PL B388 384	W. Hampel <i>et al.</i>	(GALLEX Collab.)
LOVERRE	96	PL B370 156	P.F. Loverre	
ACHKAR	95	NP B434 503	B. Achkar <i>et al.</i>	(SING, SACLD, CPPM, CDEF+)
AHLEN	95	PL B357 481	S.P. Ahlen <i>et al.</i>	(MACRO Collab.)
ATHANASSO...	95	PRL 75 2650	C. Athanassopoulos <i>et al.</i>	(LSND Collab.)
BAHCALL	95	PL B348 121	J.N. Bahcall, P.I. Krastev, E. Lisi	(IAS)
DAUM	95	ZPHY C66 417	K. Daum <i>et al.</i>	(FREJUS Collab.)
HILL	95	PRL 75 2654	J.E. Hill	(PENN)
MCFARLAND	95	PRL 75 3993	K.S. McFarland <i>et al.</i>	(CCFR Collab.)
VYRODOV	95	JETPL 61 163	V.N. Vyrodov <i>et al.</i>	(KIAE, LAPP, CDEF)
		Translated from ZETFP 61 161.		
ABDURASHI...	94	PL B328 234	J.N. Abdurashitov <i>et al.</i>	(SAGE Collab.)
DECLAIS	94	PL B338 383	Y. Declais <i>et al.</i>	
FUKUDA	94	PL B335 237	Y. Fukuda <i>et al.</i>	(Kamiokande Collab.)
SMIRNOV	94	PR D49 1389	A.Y. Smirnov, D.N. Spergel, J.N. Bahcall	(IAS+)
VIDYAKIN	94	JETPL 59 390	G.S. Vidyakin <i>et al.</i>	(KIAE)
		Translated from ZETFP 59 364.		
VILAIN	94C	ZPHY C64 539	P. Vilain <i>et al.</i>	(CHARM II Collab.)
FREEDMAN	93	PR D47 811	S.J. Freedman <i>et al.</i>	(LAMPF E645 Collab.)
GRUWE	93	PL B309 463	M.J. Gruwe <i>et al.</i>	(CHARM II Collab.)
BECKER-SZ...	92	PRL 69 1010	R.A. Becker-Szendy <i>et al.</i>	(IMB Collab.)
BECKER-SZ...	92B	PR D46 3720	R.A. Becker-Szendy <i>et al.</i>	(IMB Collab.)
BEIER	92	PL B283 446	E.W. Beier <i>et al.</i>	(KAM2 Collab.)
Also	94	PTRSL A346 63	E.W. Beier, E.D. Frank	(PENN)
BORODOV...	92	PRL 68 274	L. Borodovsky <i>et al.</i>	(COLU, JHU, ILL)
HIRATA	92	PL B280 146	K.S. Hirata <i>et al.</i>	(Kamiokande II Collab.)
KETOV	92	JETPL 55 564	S.N. Ketov <i>et al.</i>	(KIAE)
		Translated from ZETFP 55 544.		
CASPER	91	PRL 66 2561	D. Casper <i>et al.</i>	(IMB Collab.)
HIRATA	91	PRL 66 9	K.S. Hirata <i>et al.</i>	(Kamiokande II Collab.)
KUVSHINN...	91	JETPL 54 253	A.A. Kuvshinnikov <i>et al.</i>	(KIAE)
BATUSOV	90B	ZPHY C48 209	Y.A. Batusov <i>et al.</i>	(JINR, ITEP, SERP)
BERGER	90B	PL B245 305	C. Berger <i>et al.</i>	(FREJUS Collab.)
HIRATA	90	PRL 65 1297	K.S. Hirata <i>et al.</i>	(Kamiokande II Collab.)
VIDYAKIN	90	JETP 71 424	G.S. Vidyakin <i>et al.</i>	(KIAE)
		Translated from ZETF 98 764.		
AGLIETTA	89	EPL 8 611	M. Aglietta <i>et al.</i>	(FREJUS Collab.)
BAHCALL	89	Neutrino Astrophysics	J.N. Bahcall	(IAS)
		Cambridge University Press		
BLUMENFELD	89	PRL 62 2237	B.J. Blumenfeld <i>et al.</i>	(COLU, ILL, JHU)
DAVIS	89	ARNPS 39 467	R. Davis, A.K. Mann, L. Wolfenstein	(BNL, PENN+)
OYAMA	89	PR D39 1481	Y. Oyama <i>et al.</i>	(Kamiokande II Collab.)
AFONIN	88	JETP 67 213	A.I. Afonin <i>et al.</i>	(KIAE)
		Translated from ZETF 94 1, issue 2.		
AMMOISOV	88	ZPHY C40 487	V.V. Ammosov <i>et al.</i>	(SKAT Collab.)
BERGSMA	88	ZPHY C40 171	F. Bergsma <i>et al.</i>	(CHARM Collab.)
BIONTA	88	PR D38 768	R.M. Bionta <i>et al.</i>	(IMB Collab.)
DURKIN	88	PRL 61 1811	L.S. Durkin <i>et al.</i>	(OSU, ANL, CIT+)
LOVERRE	88	PL B206 711	P.F. Loverre	(INFN)
AFONIN	87	JETPL 45 247	A.I. Afonin <i>et al.</i>	(KIAE)
		Translated from ZETFP 45 201.		
AHRENS	87	PR D36 702	L.A. Ahrens <i>et al.</i>	(BNL, BROW, UCI+)
BOFILL	87	PR D36 3309	J. Bofill <i>et al.</i>	(MIT, FNAL, MSU)
LOSECCO	87	PL B184 305	J.M. LoSecco <i>et al.</i>	(IMB Collab.)
TALEBZADEH	87	NP B291 503	M. Talebzadeh <i>et al.</i>	(BEBC WA66 Collab.)
VIDYAKIN	87	JETP 66 243	G.S. Vidyakin <i>et al.</i>	(KIAE)
		Translated from ZETF 93 424.		

ABRAMOWICZ	86	PRL 57 298	H. Abramowicz <i>et al.</i>	(CDHS Collab.)
AFONIN	86	JETPL 44 142	A.I. Afonin <i>et al.</i>	(KIAE)
		Translated from ZETFP 44 111.		
ALLABY	86	PL B177 446	J.V. Allaby <i>et al.</i>	(CHARM Collab.)
ANGELINI	86	PL B179 307	C. Angelini <i>et al.</i>	(PISA, ATHU, PADO+)
BERNARDI	86B	PL B181 173	G. Bernardi <i>et al.</i>	(CURIN, INFN, CDEF+)
BRUCKER	86	PR D34 2183	E.B. Brucker <i>et al.</i>	(RUTG, BNL, COLU)
USHIDA	86C	PRL 57 2897	N. Ushida <i>et al.</i>	(FNAL E531 Collab.)
ZACEK	86	PR D34 2621	G. Zacek <i>et al.</i>	(CIT-SIN-TUM Collab.)
AFONIN	85	JETPL 41 435	A.I. Afonin <i>et al.</i>	(KIAE)
		Translated from ZETFP 41 355.		
Also	85B	JETPL 42 285	A.I. Afonin <i>et al.</i>	(KIAE)
		Translated from ZETFP 42 230.		
AHRENS	85	PR D31 2732	L.A. Ahrens <i>et al.</i>	(BNL, BROW, KEK+)
BELIKOV	85	SJNP 41 589	S.V. Belikov <i>et al.</i>	(SERP)
		Translated from YAF 41 919.		
STOCKDALE	85	ZPHY C27 53	I.E. Stockdale <i>et al.</i>	(ROCH, CHIC, COLU+)
ZACEK	85	PL 164B 193	V. Zacek <i>et al.</i>	(MUNI, CIT, SIN)
BALLAGH	84	PR D30 2271	H.C. Ballagh <i>et al.</i>	(UCB, LBL, FNAL+)
BERGSMA	84	PL 142B 103	F. Bergsma <i>et al.</i>	(CHARM Collab.)
CAVAIGNAC	84	PL 148B 387	J.F. Cavaignac <i>et al.</i>	(ISNG, LAPP)
DYDAK	84	PL 134B 281	F. Dydak <i>et al.</i>	(CERN, DORT, HEIDH, SACL+)
GABATHULER	84	PL 138B 449	K. Gabathuler <i>et al.</i>	(CIT, SIN, MUNI)
STOCKDALE	84	PRL 52 1384	I.E. Stockdale <i>et al.</i>	(ROCH, CHIC, COLU+)
AFONIN	83	JETPL 38 436	A.I. Afonin <i>et al.</i>	(KIAE)
		Translated from ZETFP 38 361.		
BELENKII	83	JETPL 38 493	S.N. Belenky <i>et al.</i>	(KIAE)
		Translated from ZETFP 38 406.		
BELIKOV	83	JETPL 38 661	S.V. Belikov <i>et al.</i>	(SERP)
		Translated from ZETFP 38 547.		
TAYLOR	83	PR D28 2705	G.N. Taylor <i>et al.</i>	(HAWA, LBL, FNAL)
COOPER	82	PL 112B 97	A.M. Cooper <i>et al.</i>	(RL)
VUILLEUMIER	82	PL 114B 298	J.L. Vuilleumier <i>et al.</i>	(CIT, SIN, MUNI)
ARMENISE	81	PL 100B 182	N. Armenise <i>et al.</i>	(BARI, CERN, MILA+)
ASRATYAN	81	PL 105B 301	A.E. Asratyan <i>et al.</i>	(ITEP, FNAL, SERP+)
BAKER	81	PRL 47 1576	N.J. Baker <i>et al.</i>	(BNL, COLU)
Also	78	PRL 40 144	A.M. Cnops <i>et al.</i>	(BNL, COLU)
BOLIEV	81	SJNP 34 787	M.M. Boliev <i>et al.</i>	(INRM)
		Translated from YAF 34 1418.		
DEDEN	81	PL 98B 310	H. Deden <i>et al.</i>	(BEBC Collab.)
ERRIQUEZ	81	PL 102B 73	O. Erriquez <i>et al.</i>	(BARI, BIRM, BRUX+)
KWON	81	PR D24 1097	H. Kwon <i>et al.</i>	(CIT, ISNG, MUNI)
NEMETHY	81B	PR D23 262	P. Nemethy <i>et al.</i>	(YALE, LBL, LASL+)
SILVERMAN	81	PRL 46 467	D. Silverman, A. Soni	(UCI, UCLA)
USHIDA	81	PRL 47 1694	N. Ushida <i>et al.</i>	(AICH, FNAL, KOBE, SEOU+)
AVIGNONE	80	PR C22 594	F.T. Avignone, Z.D. Greenwood	(SCUC)
BOEHM	80	PL 97B 310	F. Boehm <i>et al.</i>	(ILLG, CIT, ISNG, MUNI)
FRITZE	80	PL 96B 427	P. Fritze	(AACH3, BONN, CERN, LOIC, OXF+)
REINES	80	PRL 45 1307	F. Reines, H.W. Sobel, E. Pasierb	(UCI)
Also	59	PR 113 273	F. Reines, C.L. Cowan	(LASL)
Also	66	PR 142 852	F.A. Nezrick, F. Reines	(CASE)
Also	76	PRL 37 315	F. Reines, H.S. Gurr, H.W. Sobel	(UCI)
DAVIS	79	PR C19 2259	R. Davis <i>et al.</i>	(CIT)
BLIETSCHAU	78	NP B133 205	J. Blietschau <i>et al.</i>	(Gargamelle Collab.)
CROUCH	78	PR D18 2239	M.F. Crouch <i>et al.</i>	(CASE, UCI, WITW)
BELLOTTI	76	LNC 17 553	E. Bellotti <i>et al.</i>	(MILA)